Accepted Manuscript

Multi-scale records of reef development and condition provide context for contemporary changes on inshore reefs

Emma J. Ryan, Stephen E. Lewis, Scott G. Smithers, Tara R. Clark, Jian-xin Zhao

PII: S0921-8181(16)30046-7
DOI: doi:10.1016/j.gloplacha.2016.10.007
Reference: GLOBAL 2495

To appear in: *Global and Planetary Change*

Received date: 10 February 2016
Revised date: 4 October 2016
Accepted date: 6 October 2016

Multi-scale records of reef development and condition provide context for contemporary changes on inshore reefs

Authors: Emma J. Ryan[a,b,c], Stephen E. Lewis[c], Scott G. Smithers[a,c], Tara R. Clark[d], Jian-xin Zhao[d]

[a]College of Science and Engineering,
James Cook University, Townsville, QLD 4811
Australia

[b]Current Address: School of Environment,
The University of Auckland, Auckland, 1010
New Zealand

[c]Catchment to Reef Research Group, TropWATER,
James Cook University, Townsville, QLD 4811
Australia

[d]Radiogenic Isotope Facility, School of Earth Sciences
The University of Queensland, Brisbane, QLD 4072
Australia

Corresponding author: Emma J. Ryan e.ryan@auckland.ac.nz

ABSTRACT

Comparisons between historical and contemporary photographs of coral reef flats from the inshore Great Barrier Reef (GBR) have been cited by various authors and agencies as evidence of reef degradation since European settlement and have been presented as proof of widespread reef decline. The diminished condition is inferred from reduced live coral cover and structural diversity depicted in the contemporary photographs. Anthropogenic causes for this deterioration are most often proposed, usually because it is argued to have coincided with modifications to coastal catchments by European settlers. However, changes in reef condition inferred from photographic comparisons have rarely been verified against quantitative assessments of reef geomorphic state or current reef status. Photographs taken in the late 1800s of the reef flat at Stone Island, located in Edgecumbe Bay in the inshore central GBR, have been compared by others with more recent images to interpret significant reductions in coral cover and diversity over the past 120 or so years. We examined the internal structure of fringing reefs at two locations on Stone Island by collecting 14 percussion cores across the reef flats. Sedimentological analyses coupled with uranium-thorium dating allowed for the reconstruction of reef development over the past ~7,000 years. Both reefs at Stone Island initiated prior to 7,000 calendar years before present (yBP, where present is 1950 AD) and both reef flats were almost entirely emplaced by 4,000 yBP. Surveys of the benthic ecology of reefs at Stone Island and at Middle Island, also in Edgecumbe Bay, indicate that coral cover and diversity across reef flats and slopes was patchy and varied spatially within each location and throughout the region. Live coral cover on the Middle Island reef flat reached an average (± 1σ standard deviation) of 63.1 ± 20.2%. This was much higher than the live coral cover at Stone Island, where only a few small living coral colonies were recorded. We evaluate the use of photographic records from Stone Island to depict regional changes in reef condition by comparing the trends in reef condition determined from photographic records with underlying reef geomorphic state reconstructed from reef cores. We conclude that inferred changes in reef condition at Stone Island are localised and should not be used as evidence of widespread regional decline on the GBR.

KEY WORDS

Great Barrier Reef; reef cores; chronostratigraphy; U-Th dating; Stone Island; Middle Island

1. Introduction

Major declines in live coral cover have been documented on coral reefs globally over the past four decades (Gardner et al. 2003; Bruno and Selig, 2007; Wilkinson, 2008; De'ath et al. 2012). Anthropogenic stressors such as over-fishing (Hughes et al. 2007), contaminants, and elevated sediment loads exported from modified catchments (Fabricius, 2005) have been linked to ecological phase-shifts on coral reefs, whereby a coral-dominated ecosystem is transformed into a macroalgae-dominated ecosystem with relatively few hard corals (Hughes, 1994; Bellwood et al. 2004). Shifts in the dominant coral taxa on reefs have also been reported, towards dominance of non-framework building corals (Perry et al. 2015) or opportunistic taxa (Green et al. 2008; Alvarez-Filip et al. 2011). However, the global magnitude and regional extent of such phase-shifts is not well documented or understood (Bruno et al. 2009) and some coral reefs have experienced long periods of recovery while being exposed to human influences (Maragos et al. 1985; Kittinger et al. 2011; Gilmour et al. 2013). Furthermore, how shifts in reef condition forced by human activities interplay with those produced by natural disturbances is also poorly understood. On the Great Barrier Reef (GBR) of Australia, inshore reefs (usually defined as those situated within the 20 m isobath and the mainland coast [Hopley et al. 2007]) are considered most susceptible to ecological phase-shifts due to their proximity to modified coastal catchments and river discharge (Fabricius et al. 2005; Browne et al. 2012; Waterhouse et al. 2012). Since European settlement of the Queensland coast in the early-mid 19th Century, sediment, nutrient and pollutant loads exported to the GBR lagoon have increased two- to ten-fold (McCulloch et al. 2003; Kroon et al. 2012; Waters et al. 2014) and high floods in coastal rivers have become more frequent, increasing from 1 in 20 years prior to European settlement to 1 in 6 years (Lough et al. 2015). However, direct evidence of the impact these changes have on inshore reefs is lacking and whether they are localised or system-wide is contested (see Sweatman et al. 2011; Hughes et al. 2011; Sweatman and Syms, 2011).

Evidence for coral loss on inshore reefs of the GBR is largely derived from reef monitoring studies undertaken across a wide range of reefs on the GBR since the 1980s (e.g. Done et al. 2007; Thompson and Dolman, 2010; De'ath et al. 2012). These ecological data collected over decades are enormously valuable for informing management, but nonetheless provide very restricted temporal records of reef condition compared to those preserved in historical sources (Thurstan et al. 2015) and the fossil record (Pandolfi and Kiessling, 2014), which for most inshore reefs on the GBR may encompass several millennia (Smithers et al. 2006). Historical and contemporary photographs of reef flats have been compared to determine changes in coral cover and structure on inshore reefs over a 'longer-term' centennial-scale period (Wachenfeld, 1997). In 1994, Wachenfeld (1997) attempted to replicate the historical photographs of Stone Island reef flat taken by Saville-Kent (1893) at low tide (shown in Fig. 1); Wachenfeld's 1994 photographs depict a conspicuous change from a coral-dominated reef flat in the late 1800s/early 1900s to a macroalgae- and sediment-dominated reef flat. More recent photographs taken in 2012 by Clark et al. (2016) and those in Fig. 1 show this condition persists (see also Electronic Supplementary Materials 1). The sequence of photographs from Stone Island have been broadly used as evidence of widespread reef degradation in the inshore GBR (Hughes et al. 2010; Bell et al. 2014; GBRMPA 2013, 2014; Hoegh-Guldberg, 2014), despite Wachenfeld (1997, pp. 147) concluding that the results from the historical photograph project "…throws doubt on the proposition that the GBR is subject to broad scale decline". Of the 14 reefs examined by Wachenfeld (1997) just 4 reefs displayed major change between the late 1880s and 1994, including Stone Island and nearby Bramston Reef. Interestingly, a recent study by Ryan et al. (2016a) suggested that the reef flat condition at Bramston Reef in 2013 was not dissimilar to descriptions of Bramston Reef given by Saville-Kent (1893). This raises concerns with the validity of the photographic comparison that were originally emphasised by Wachenfeld (1997) and remain unresolved today, including: 1) a single photograph from one location on a reef flat may not be representative of the entire reef flat; and 2) each photograph captures just one point in time and does not provide sufficient temporal resolution, given the dynamic nature of coral cover across reefs, and especially across reef flats. Furthermore, it is likely that the original photographs taken by Saville-Kent were deliberately taken in areas of high benthic cover. Indeed, Saville-Kent (1893) stated intentions for the photographs to be used to monitor future coral growth. In addition, the elevation of the reef flat at the location where the historical and contemporary photographs were taken is not properly referenced to a tidal datum (with the exception of recent work by Clark et al. [2016]) and thus the possible influence of the elevation of these commonly emergent reef flats cannot be determined. Accordingly, firm conclusions about regional-scale inshore reef condition should not be drawn from historical photographic evidence alone and quantitative baseline data on contemporary and past (centennial-millennial scale) reef condition (which do not currently exist at Stone Island) are required.

When used together with quantitative data about past and present reef state, historical and contemporary photographs may provide additional supplementary evidence of changes in reef condition.

Long-term reef growth records provide valuable baseline knowledge about past reef development, condition and variability throughout the Holocene (Smithers et al. 2006). On the GBR, records of long-term reef growth have revealed that many inshore reefs began to develop in the early- to mid-Holocene some 7,000 years ago and reef flats were established within 1,000–3,000 years of initiation (Smithers et al. 2006; Perry and Smithers, 2010; Roche et al. 2011; Ryan et al. 2016b) under a relative mean sea level that was around 1 m higher than present (Lewis et al. 2013). Late-Holocene sea-level fall, the precise timing and nature of which remains debated (Perry and Smithers, 2011; Lewis et al. 2015), has exposed the older, back areas of these reef flats that are now elevated above the level of modern reef flat formation (Kleypas, 1996; Smithers et al. 2006). Not only are long-term reef growth studies rare, they are seldom considered in assessments of contemporary reef condition despite their ability to provide valuable baseline knowledge.

Here, we present data over multiple timeframes (millennial-centennial-present) to assess the use of historical and contemporary photographic comparisons from Stone Island as indicators of regional inshore reef decline. We incorporate evidence from descriptions and photographs of reef flat condition collected since ~1890 AD that exist for the fringing reefs in Edgecumbe Bay (Stone Island, Middle Island and Bramston Reef, Fig. 2), with a focus on Stone Island. The Holocene development of fringing reefs at Stone Island is determined using uranium-thorium (U-Th) dated corals from percussion cores and fossil microatolls. Chronostratigraphic records detail the timing and mode of reef growth and reef flat development, as well as the reef sediment matrix and palaeo-ecology that comprised Stone Island reef in the past. The contemporary geomorphology, benthic cover and distribution are also quantified, with high-precision elevation control, at two fringing reefs at Stone Island and the fringing reef at Middle Island.

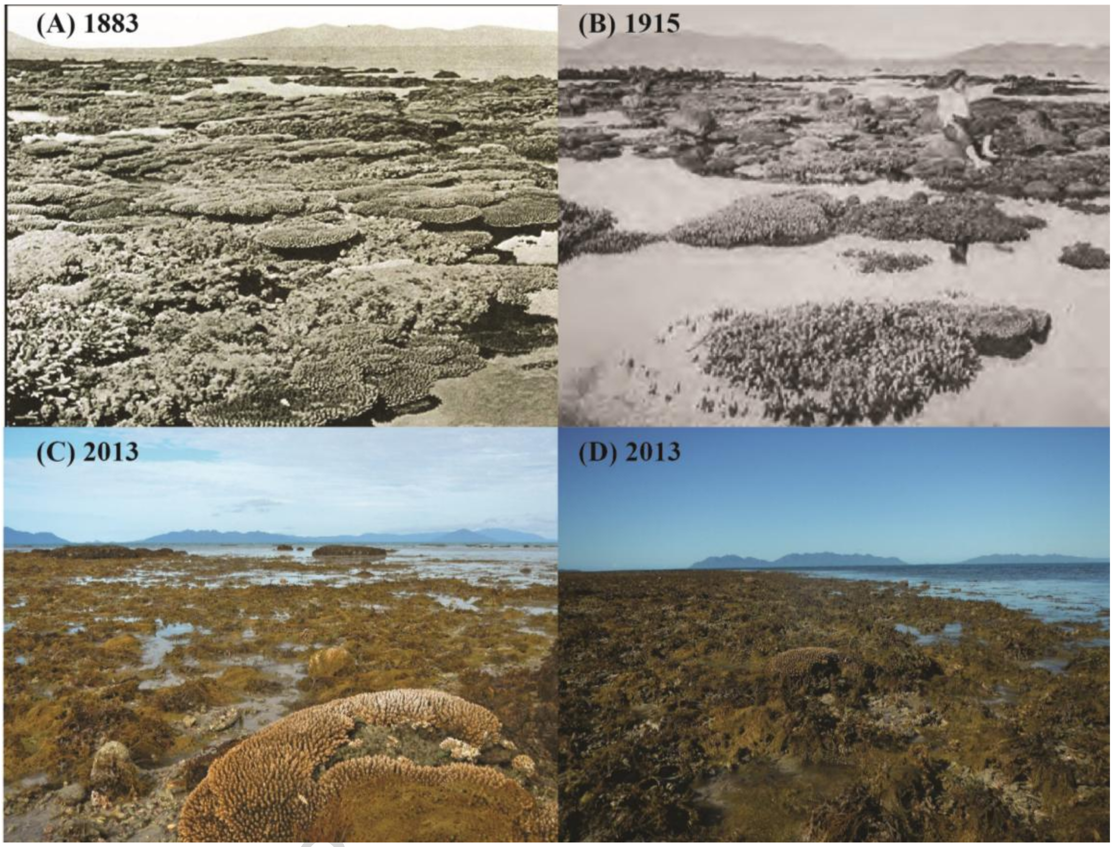

Fig. 1. Photographs of the Stone Island reef flat: (A) taken by Saville-Kent (1893) in 1883, (B) taken in 1915 by an unknown photographer, (C) and (D) taken by E. Ryan at spring low tides (0.13 and 0.23 m above lowest astronomical tide on 22 (C) and 21 (D) July 2013, respectively). Note the high standing fossil microatolls at the water's edge in (C). For additional photographs and elevations of the reef flat surface where photographs were taken see Electronic Supplementary Materials 1.

2. Regional Setting

Stone Island (20°02'S, 148°17'E) and Middle Island (19°59'S, 148°22'E) are located 3 km and 10 km offshore from Bowen in Edgecumbe Bay, respectively (Fig. 2A). Stone Island is located in the inshore turbid zone where surrounding waters are <6 m deep, while Middle Island is situated on the inner-mid shelf margin in waters ~16 m deep. Stone Island is fringed by two reefs: one located on the windward, south-eastern side of the island (Stone Island South [SI-S]) with a ~450 m wide reef flat, and one located in Shoalwater Bay on the northern side of the island (Stone Island North [SI-N]) with a ~400 m wide reef flat (Fig. 2C). SI-S is the larger of the reefs on Stone Island, extending around 1.5 km alongshore. On the southern side of Middle Island a reef flat as much as 330 m wide extends along ~600 m of shoreline (Fig. 2B). The reefs at Stone Island and Middle Island experience a semi-diurnal tidal regime with a spring tidal range around 3.6 m where reef flats at both islands are largely exposed at lower tidal stages. A ~400 m long sand spit has developed at the western extent of the SI-S reef flat (Fig. 2C), indicating that waves and currents generated by prevailing south-easterly trade winds predominantly transport sediment to the north-west. This occurs even though both Middle and Stone Islands are relatively protected from swells generated by the dominant south-east trade winds by Gloucester Island and Cape Gloucester.

Rainfall, tropical cyclones and high river flows are very seasonal in the Queensland dry tropics, usually restricted to the warmer months (December to March). Interannual variation can also be significant, and is strongly influenced by El Niño Southern Oscillation and Pacific Decadal Oscillation conditions (Rodriguez-Ramirez et al. 2014). As a result, freshwater and sediment discharge to the inshore GBR are highly variable seasonally and inter-annually. Terrestrial sediment input to Edgecumbe Bay is largely from the Proserpine Basin, which is a 2,535 km^2 modified catchment (over 50% dedicated to grazing; Packett et al. 2014). The Gregory River (Fig. 2) and several minor creeks (Duck Creek, Eden Lassie Creek, Greta Creek and Billy Creek) discharge directly into Edgecumbe Bay, while the Don River mouth lies 9 km to the north of Stone Island. Major river mouths are located >80 km away from Edgecumbe Bay, with the Burdekin River ~80 km to the north and the O'Connell River ~120 km to the south.

Europeans settled in Bowen ~1861 AD (McIntyre-Tamwoy, 2004) and began to modify the landscape on Stone Island soon after. In contrast, Middle Island has been largely untouched by Europeans. At Stone Island, sheep and goats were introduced in the late 19th and early 20th Centuries (Bowen Independent, 1916, 1934), a tourist resort was developed on the island during the mid-20th Century, and a 23-acre lake was dammed in the centre of the island to create a freshwater supply in 1972 (Bartram, 1972). Although the tourist resort has closed, infrastructure and roads remain. Dredging in Edgecumbe Bay began in 1886 to develop the Bowen shipping channel and jetty (Steen, 1972) but no data are available to assess the impacts of dredging on the hydrodynamics and sediment movement within the bay. Brodie et al. (2014) suggested nearshore areas of Edgecumbe Bay were poorly flushed based on hydrodynamic modelling (Andutta et al. 2013), however the model used was not specifically developed for Edgecumbe Bay and no field data exist to validate the model results.

Excellent historical descriptions and photographs exist for Stone Island (Saville-Kent, 1893) and Middle Island (Agassiz, 1898), which establish that the reef flats at both islands were in good condition in the late 1800s. Saville-Kent's detailed descriptions include several photographs of the reef flat at SI-S taken during spring low tide (location revealed by Hedley [1925]) that show high coral cover, including *Madrepora (Acropora), Montipora, Goniastraea grayi (Goniastrea pectinata), Turbinaria cineraseeus* and *Losphoseris (Pavona) cristata* (Saville-Kent, 1893). In 1896 the outer face of Middle Island's reef flat was "coated with fine heads of corals… becoming less prominent as they tend towards the shallower edge of the flat" (Agassiz, 1898, pp. 107). However, by the 1920s no trace of living coral was documented at either Stone or Middle Island (Hedley, 1925; Rainford, 1925). Two cyclones in 1918 caused high rainfall and a large freshwater plume, which in concert with low spring tides and northerly winds are argued to have caused total mortality of the reef flats (Hedley, 1925; Rainford, 1925). Stanley (1928) reported that in June 1925 live coral cover at Stone Island was recovering and small colonies of *Goniastrea, Merulina, Turbinaria, Fungia* and soft corals were flourishing. Stanley (1928) refers to both the 'extensive fringing reef to the south' (presumably the SI-S reef) and the reef in Shoalwater Bay but does not specify which reef was recovering in the mid-1920s. In 1936 the reef flats at Stone Island and Middle Island were "dead on their upper surfaces" (Steers, 1937) and negligible recolonisation of coral had occurred by 1953 (Stephenson et al. 1958). According to anecdotal evidence in Wachenfeld, (1997), the reef flat at SI-S was apparently in good condition in the 1970s. In contrast, Hopley (1975), who conducted the first comprehensive geomorphological investigation at Middle

Island described the reef flat there during the same period as 'largely dead'. Although these sites in Edgecumbe Bay have detailed historical records that provide snapshots of reef condition over the past century or so, a longer-term perspective on reef development and disturbance/recovery regimes has to date not been established and used as context for interpreting recent changes.

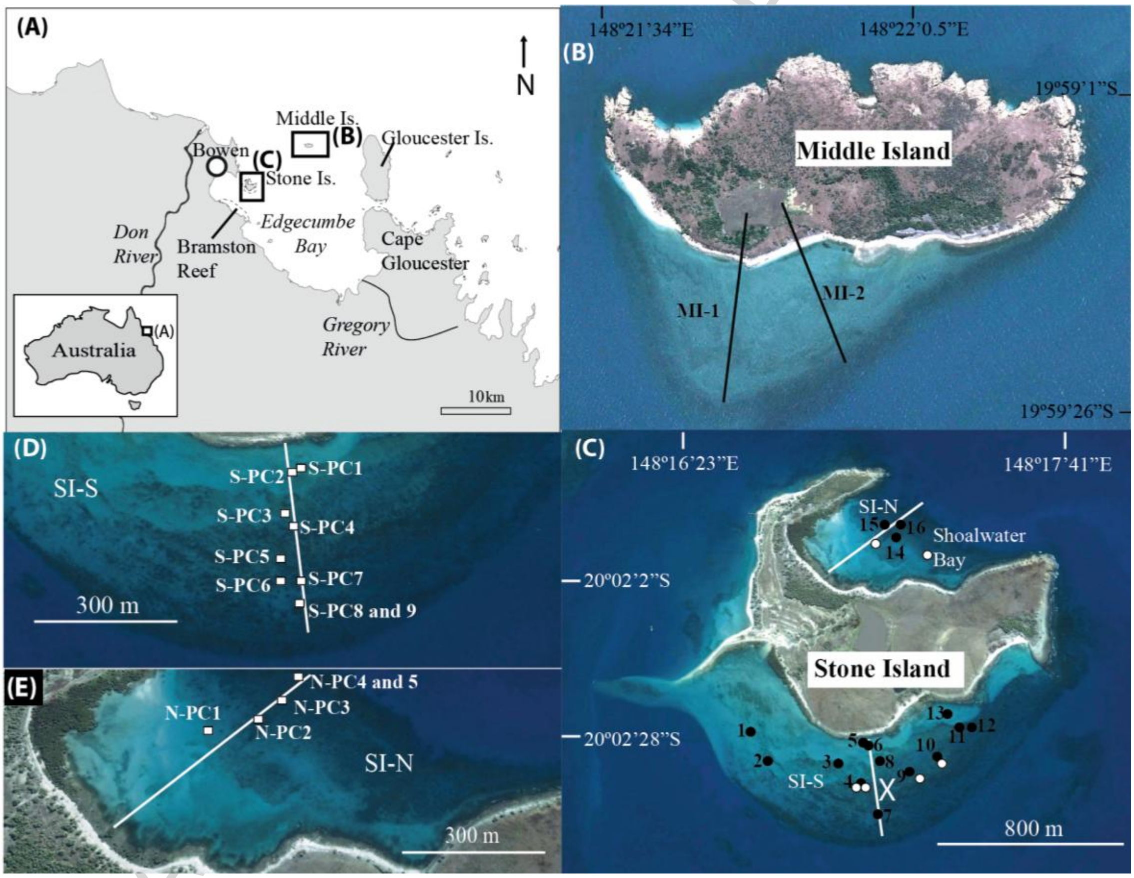

Fig. 2. (A) Location of Stone Island, Middle Island and Bramston Reef in Edgecumbe Bay, Australia; (B) the reef flat and transects one (MI-1) and two (MI-2) at Middle Island; (C) the reef flats at Stone Island South (SI-S) and Stone Island North (SI-N). Fossil microatolls (numbered 1-16) are shown by black dots and living open-water microatolls are shown by white dots. The approximate location of the photographs taken by Saville-Kent (1893) and Wachenfeld (1997) is shown by the white X; (D) the location of percussion cores (white squares) on the transect at SI-S; and (E) the location of percussion cores (white squares) on the transect at SI-N.

3. Materials and Methods

Field studies were conducted in the austral winters of 2013 and 2014 during low spring tides (<0.5 m above lowest astronomical tide [LAT] during the day). All location and elevation data were collected using a Trimble Real Time Kinematic (RTK) Global Positioning System

(GPS) with the vertical and horizontal precision being ~0.01–0.005 m. The high-precision elevation data were reduced to LAT relative to datum RTK GPS base station values obtained from AUSPOS 2.1 (an online GPS processing service) allowing accurate inter- and intra-site comparisons.

3.1 Past reef development

3.1.1 Percussion cores

To examine Holocene reef development at Stone Island, nine reef cores were collected from SI-S and five from SI-N using the percussion coring technique described in Perry and Smithers (2006). The cores were collected along shore-perpendicular transects on the reef flat (Fig. 2D,E) ensuring cores were spread across the width of the reef flat and throughout all geomorphic zones where logistically possible. The number of cores collected was a function of the width of the reef flat and the time available in the field. Cores between 1.2 and 5.1 m long extended from the reef flat surface vertically into the reef structure (Fig. 3) and captured reef framework, detrital material and reef matrix sediments. Total compaction rates across the cores from both reef flats varied between 19–45%. The compaction rate in core S-PC3 below 2.0 m downcore was 59% due to a coral clast that was wedged in the core at 2.0 m depth.

In the laboratory, each core was halved lengthways and visually logged to record downcore changes in the type and preservation of reef framework material and the type and size of matrix sediments. The core logs were used to differentiate facies that had similar reef framework material and matrix composition. Sediment samples (~20 g) were taken from the cores at 20 cm (uncompacted) downcore intervals and analysed for grain size, carbonate content and mud content using sieving, Rapid Sediment Analyser and acid digestion techniques described in Ryan et al. (2016a). Palaeo-ecological descriptions were also conducted on each core using the method in Ryan et al. (2016a) where corals were grouped and weighed according to the genus. Veron (1986), Coral Finder 2.0 (Kelley, 2009) and Budd et al. (2012) were used for coral identification. If corals were unidentifiable to genus level due to poor preservation and/or encrustation they were grouped as unidentified and classified as rubble. Note that sediment and palaeo-ecological analyses were not performed on S-PC3 below 2.0 m downcore due to the high compaction rate.

3.1.2 Fossil microatoll samples

The elevations of un-moated fossil *Porites* microatolls of known age can be compared with the elevation of modern living equivalents to reconstruct past sea levels (Chappell et al. 1983; Smithers and Woodroffe, 2000). In addition, fossil microatoll ages document the timing of reef flat development and lateral accretion rates. The locations and surface elevations of fossil microatolls (mainly *Porites*) were surveyed using the RTK GPS. A small coral core sample (~4 cm long, 2 cm diameter) was extracted from the surface rim of 16 fossil microatolls using a brace and bit hand drill. Each fossil microatoll sample was dated using U-Th techniques (detailed in section 3.1.3) to determine the colony age. Ten fossil microatoll samples from the Middle Island reef flat were collected and dated by Ryan et al. (2016b) using the techniques described here.

3.1.3 U-Th dating

Well-preserved corals were selected from the cores for dating to reconstruct detailed chronostratigraphies for the reefs examined. Corals selected were regarded as *in situ* due to well-preserved delicate skeletal structures and the upward positioning and orientation of corallites. The core samples and fossil microatoll samples were vigorously cleaned and prepared for dating using techniques described in Ryan et al. (2016a) and Clark et al. (2014a). Samples were U-Th dated at The University of Queensland using a Nu Plasma multi-collector inductively coupled plasma mass-spectrometer (MC-ICP-MS). U-Th dating procedures used were similar to those described in detail in Zhao et al. (2001) and Clark et al. (2014a, 2014b). Ages are presented as calendar years before present (yBP), where present is defined as 1950 AD.

3.2 Contemporary geomorphology and benthic cover

RTK GPS surveys of reef flat topography were undertaken across shore-perpendicular transects (Fig. 2B,C). Eco-geomorphological zones were differentiated along transects based on variations in reef flat elevation, coral cover, sediment type, morphological features and algae/seagrass cover. In each eco-geomorphological zone, five 1 m^2 quadrats were randomly placed when the reef flat was exposed at low tidal stages and photographed with a digital camera. To photograph the reef slope (which was not exposed at low tide) spatially-referenced video photography was captured across seaward extensions of the transects that extended to the base of the reef slope using an underwater SeaViewer drop camera paired with a Trimble Juno GPS. Between 16 and 36 still images were extracted from the video footage of each slope transect, according to the number of geomorphological zones identified, the transect length and the benthic variation within each zone. At Stone Island, reef slope depth was estimated using a depth sounder and calibrated against predicted tides to reduce depths to LAT.

Substrate composition was determined from the reef flat quadrat photographs and still images extracted from the video footage using Coral Point Count with Excel Extensions (CPCe) software (Kohler and Gill, 2006). The substrate was quantified based on the proportional cover of various substrates (sand, rubble, shell, reef pavement/framework), live coral and vegetation (algae and seagrass) using the stratified random point count method in CPCe, following Browne et al. (2010) and Ryan et al. (2016a). The average percent composition for each zone was calculated. Where possible live corals were identified to genus. However, if poor image quality and/or turbid water conditions prevented confident identification, which was often the case, corals were classified according to their structural morphology (i.e. branching, massive, plate, foliaceous, columnar, encrusting or free-living).

4. Results

4.1 Holocene reef development at Stone Island

The chronostratigraphy was inferred for each Stone Island reef from the percussion cores, fossil microatoll samples and U-Th ages (Fig. 3). All U-Th ages from core and fossil microatoll samples are presented in Table 1. The chronostratigraphies reveal details about the timing and mode of reef development, the reef palaeo-ecology and the reef matrix sediments. The cores from the two reefs captured up to 5 m of reef framework and matrix and did not reach the pre-reefal surface, indicating the entire Holocene thickness of each reef is >5 m. Given the water depth immediately seaward of the reef slope is ~6–7 m, the pre-reefal surface is probably ~6–6.5 m below the present surface, and thus we are confident that the percussion cores captured the majority of the reef structure.

4.1.1 Reef facies

Four reefal facies were differentiated in the cores collected at SI-S and SI-N: facies A, B, C and D (Table 2; Electronic Supplementary Materials 2). For both Stone Island reefs, the matrix sediments generally coarsen upwards, as the mud fraction (<63 μm) in the cores decreased towards the surface to a minor component (4.2 ± 2.0% [mean ± 1 standard deviation] or 9.6 ± 5.2%) and medium-coarse carbonate sands (grain size 2000–250 μm) dominated (96.9 ± 2.3% carbonate in facies A, Table 2). Mud-containing facies dominated the cores from SI-S (mud content up to 47.8 ± 13.9% in facies D), comprising all but the uppermost metre or so of the cores. A lower mud content characterised facies in SI-N cores;

the muddiest facies C contained 20.7 ± 5.3% mud. Throughout the cores, carbonate sediments dominated (>70%), with terrigenous fractions that were higher in SI-S cores (24.6 ± 7.9 and 29.5 ± 9.5% in facies C and D, respectively) than SI-N cores (18.3 ± 9.7% in facies C). Coral clasts (framework and detrital material), shell hash and disarticulated bivalves were recovered amongst the sediment matrix throughout all cores. Coral clasts were generally rubble, derived from branching corals; some were heavily encrusted with coralline algae and others were well-preserved. In addition, echinoderm spines (some remarkably well-preserved) were recovered in S-PC6.

4.1.2 Palaeo-ecology

Well-preserved coral material from 28 different coral genera was recovered in the cores collected across SI-S and SI-N, however most material was so encrusted and/or abraded that accurate identification was not possible (such clasts were classified as 'unidentified rubble'). Identified coral genera were: *Acropora, Anacropora, Astreopora, Australogyra, Calaustrea, Cyphastrea, Dipsastraea, Echinophyllia, Echinopora, Euphyllia, Favites, Fungia, Galaxea, Goniastrea, Hydnophora, Isopora, Lobophyllia, Montipora, Oxypora, Pachyseris, Pavona, Platygyra, Porites, Psammocora, Seriatopora, Stylophora, Tubastrea* and *Turbinaria*. The dominant framework contributors (e.g. *Acropora, Porites, Montipora, Goniastrea, Galaxea*) were found in the cores from both sites, however five genera were unique to cores from SI-S (*Anacropora, Echinophyllia, Favites, Psammocora* and *Tubastrea*) and eight genera were unique to cores from SI-N (*Australogyra, Calaustrea, Echinopora, Dipsastraea, Isopora, Lobophyllia, Oxypora* and *Platygyra*). Spiculite clusters produced by soft corals were only recovered in cores from SI-N.

Table 1. MC-ICP-MS U-Th data from microatoll and percussion core coral samples from Stone Island, central GBR.

Sample Name	Sample genus	Sample weight (g)	U (ppm)	^{232}Th (ppb)	(^{230}Th/ ^{232}Th)	(^{230}Th/^{238}U)	(^{234}U/ ^{238}U)	uncorr. ^{230}Th Age (ka)†	corr. ^{230}Th Age (ka)	corr. Initial (^{234}U/ ^{238}U)	Age (years BP=1950)
S-1	*Montipora*	0.21575	3.1467±0.0026	19.427±0.020	34.336±0.071	0.06987±0.00014	1.14306±0.00082	6.869±0.015	6.746±0.029	1.14600±0.00084	6681±29
S-2	*Acropora*	0.21053	3.0082±0.0016	4.9554±0.0056	137.20±0.27	0.07449±0.00013	1.14539±0.00091	7.323±0.014	7.287±0.016	1.14847±0.00092	7222±16
S-3	*Montipora*	0.19953	3.1606±0.0016	12.210±0.017	57.45±0.13	0.07314±0.00014	1.14460±0.00094	7.191±0.015	7.113±0.022	1.1477±0.0010	7048±22
S-4	*Acropora?*	0.20736	3.9607±0.0027	24.873±0.030	34.51±0.10	0.07142±0.00019	1.14569±0.00093	7.010±0.020	6.886±0.032	1.14874±0.00094	6821±32
S-5	*Acropora?*	0.17518	3.1187±0.0018	13.6891±0.0091	49.90±0.11	0.07218±0.00016	1.14604±0.00081	7.085±0.017	6.996±0.024	1.14909±0.00082	6931±24
S-6	*Galaxea*	0.16176	3.3103±0.0018	3.7376±0.0051	192.51±0.52	0.07163±0.00017	1.1475±0.0011	7.020±0.018	6.994±0.019	1.1505±0.0011	6929±19
S-7	*Fungia*	0.24719	3.1007±0.0018	4.1694±0.0042	141.86±0.35	0.06287±0.00015	1.14596±0.00093	6.146±0.016	6.116±0.017	1.14855±0.00095	6051±17
S-8	*Acropora*	0.15603	3.4518±0.0032	16.577±0.016	41.449±0.071	0.06561±0.00011	1.1442±0.0010	6.431±0.013	6.335±0.023	1.1470±0.0010	6270±23
S-9	*Acropora*	0.19332	3.8507±0.0019	14.213±0.039	55.14±0.19	0.06707±0.00015	1.14667±0.0086	6.564±0.015	6.490±0.021	1.14950±0.0088	6425±21
S-10	*Goniastrea?*	0.16593	2.7815±0.0017	10.348±0.011	61.31±0.14	0.07517±0.00016	1.1460±0.0010	7.388±0.017	7.312±0.023	1.1491±0.0010	7247±23
S-11	*Acropora*	0.18877	3.4118±0.0013	16.349±0.014	29.254±0.061	0.046201±0.000091	1.1456±0.0011	4.485±0.010	4.389±0.022	1.1476±0.0011	4324±22
S-13	*Porites?*	0.21903	2.8464±0.0018	1.1778±0.0014	336.86±0.79	0.045941±0.000098	1.1447±0.0011	4.463±0.011	4.450±0.011	1.1466±0.0012	4385±11
S-15	*Turbinaria*	0.1513	3.7116±0.0023	9.5592±0.0091	77.19±0.18	0.06552±0.00015	1.1449±0.0011	6.419±0.016	6.366±0.019	1.1476±0.0011	6301±19
S-17	*Dipsastraea?*	0.15749	2.4786±0.0015	13.976±0.016	37.779±0.076	0.07021±0.00013	1.1442±0.0010	6.896±0.014	6.783±0.026	1.1472±0.0010	6718±26
S-18	*Cyphastrea*	0.21055	2.68441±0.00078	4.2976±0.0041	133.36±0.27	0.07036±0.00013	1.1441±0.0010	6.913±0.014	6.877±0.016	1.1470±0.0011	6812±16
S-19	*Turbinaria*	0.1553	3.3376±0.0023	4.9700±0.0055	115.97±0.29	0.05692±0.00014	1.14558±0.00084	5.551±0.014	5.519±0.016	1.14791±0.00085	5454±16
S-20	*Acropora*	0.18981	3.3703±0.0014	15.703±0.035	46.18±0.14	0.07092±0.00016	1.14390±0.00059	6.970±0.017	6.877±0.025	1.14687±0.00060	6812±25
S-21	*Montastrea?*	0.16615	2.7145±0.0015	8.4770±0.0080	44.72±0.12	0.04603±0.00012	1.1443±0.0010	4.473±0.013	4.408±0.018	1.1462±0.0010	4343±18
S-22	*Acropora*	0.19371	3.2528±0.0018	4.9628±0.0099	114.54±0.39	0.05760±0.00016	1.14552±0.00083	5.620±0.017	5.586±0.018	1.14789±0.00085	5521±18
S-23	*Galaxea*	0.15815	3.0829±0.0019	5.3853±0.0052	126.84±0.27	0.07302±0.00015	1.14651±0.00056	7.167±0.015	7.129±0.017	1.14955±0.00057	7064±17
S-24	*Montipora*	0.16677	3.3881±0.0015	18.564±0.024	35.775±0.087	0.06460±0.00014	1.1436±0.0011	6.333±0.015	6.224±0.026	1.1463±0.0011	6159±26
S-34	*Echinophyllia?*	0.16562	2.9049±0.0015	6.4259±0.0063	99.32±0.22	0.07241±0.00015	1.14382±0.00079	7.122±0.016	7.075±0.018	1.14680±0.00081	7010±18
S-35	*Astreopora*	0.16991	2.8840±0.0018	10.662±0.017	60.40±0.18	0.07359±0.00019	1.1466±0.0013	7.224±0.021	7.148±0.026	1.1497±0.0013	7083±26
S-36	*Acropora*	0.15099	3.3960±0.0019	4.7758±0.0053	115.53±0.28	0.05355±0.00012	1.1459±0.0010	5.213±0.013	5.182±0.014	1.1481±0.0010	5117±14
S-37	*Hydnophora*	0.17439	2.9422±0.0015	11.349±0.011	39.43±0.10	0.05012±0.00012	1.14721±0.00095	4.867±0.012	4.788±0.020	1.1493±0.0010	4723±20
SI-S-FMA-1	*Porites*	0.1556	3.0897±0.0017	4.1796±0.0035	104.75±0.27	0.046700±0.00012	1.14746±0.00091	4.527±0.012	4.497±0.014	1.14939±0.00092	4432±14
SI-S-FMA-2	*Porites*	0.2076	2.7754±0.0015	2.2285±0.0026	151.06±0.44	0.03998±0.00011	1.14503±0.00081	3.872±0.011	3.852±0.012	1.14665±0.00081	3787±12

SI-S-FMA-3	*Porites*	0.17588	2.88401±0.00094	6.102±0.011	96.77±0.26	0.06748±0.00014	1.1431±0.0014	6.628±0.016	6.582±0.019	1.1458±0.0014	6518±19
SI-S-FMA-4	*Porites*	0.16906	3.0751±0.0018	5.2987±0.0071	122.11±0.39	0.06934±0.00020	1.1427±0.0010	6.818±0.021	6.780±0.023	1.1455±0.0010	6716±23
SI-S-FMA-5	*Porites*	0.17473	3.4858±0.0013	0.31911±0.00057	2058.90±5.20	0.06211±0.00011	1.1422±0.0012	6.090±0.013	6.084±0.013	1.1447±0.0013	6020±13
SI-S-FMA-6	*Porites*	0.16148	2.8541±0.0017	8.195±0.014	73.18±0.22	0.06926±0.00018	1.1431±0.0013	6.807±0.020	6.747±0.23	1.1459±0.0014	6683±23
SI-S-FMA-7	*Porites*	0.16971	2.9055±0.0012	5.982±0.018	90.33±0.39	0.06132±0.00019	1.1437±0.0010	6.002±0.020	5.958±0.022	1.1462±0.0011	5894±22
SI-S-FMA-8	*Porites*	0.24771	2.9610±0.0014	6.9935±0.0089	87.92±0.24	0.06844±0.00017	1.1449±0.0010	6.713±0.018	6.663±0.021	1.1478±0.0011	6599±21
SI-S-FMA-9	*Porites*	0.16688	3.0193±0.0013	26.660±0.033	25.522±0.071	0.07427±0.00019	1.1394±0.0011	7.341±0.021	7.167±0.040	1.1425±0.0011	7103±40
SI-S-FMA-10	*Porites*	0.21337	2.8451±0.0021	2.0915±0.0043	288.51±0.94	0.06990±0.00018	1.14483±0.00087	6.861±0.019	6.842±0.020	1.14768±0.00088	6777±20
SI-S-FMA-11	*Porites*	0.16964	2.6623±0.0019	4.3082±0.0044	132.76±0.26	0.07081±0.00013	1.14465±0.00094	6.954±0.014	6.918±0.016	1.1476±0.0010	6853±16
SI-S-FMA-12	*Porites*	0.23411	2.7961±0.0012	8.8096±0.0080	64.68±0.15	0.06717±0.00015	1.14556±0.00067	6.581±0.016	6.516±0.020	1.14836±0.00068	6451±20
SI-S-FMA13	*Porites*	0.16273	2.8711±0.0021	11.670±0.013	51.79±0.13	0.06937±0.00016	1.1438±0.0010	6.815±0.017	6.732±0.024	1.1466±0.0010	6667±24
SI-N-FMA-14	*Porites*	0.1689	2.7336±0.0016	29.764±0.036	13.625±0.039	0.04890±0.00013	1.1453±0.0010	4.754±0.013	4.540±0.045	1.1475±0.0010	4475±45
SI-N-FMA-15	*Porites*	0.18224	2.7080±0.0015	1.8490±0.0022	100.60±0.37	0.022638±0.000080	1.14625±0.00089	2.1743±0.0080	2.1560±0.0088	1.14717±0.00089	2091±9
SI-N-FMA-16	*Porites*	0.1687	2.6780±0.0014	10.875±0.011	16.870±0.078	0.02258±0.00010	1.1478±0.0011	2.165±0.010	2.083±0.019	1.1488±0.0011	2018±19

Ratios in parentheses are activity ratios calculated from atomic ratios using decay constants of Cheng et al. (2000). All values have been corrected for laboratory procedural blanks. All errors reported as 2σ. Uncorrected ^{230}Th age was calculated using Isoplot/EX 3.0 program (Ludwig, 2003), where *ka* denotes thousand years.

†^{230}Th ages corrected using a model two-component correction value based on the equation from Clark et al. (2014b):

$$\left(\frac{^{230}Th}{^{232}Th}\right)_{mix} = \left(\left(\frac{^{232}Th_{live}}{^{232}Th_{dead}}\right)\times\left(\frac{^{230}Th}{^{232}Th}\right)_{live}\right) + \left(\left(\frac{^{232}Th_{dead} - ^{232}Th_{live}}{^{232}Th_{dead}}\right)\times\left(\frac{^{230}Th}{^{232}Th}\right)_{sed}\right)$$

where $^{232}Th_{dead}$ is the measured ^{232}Th value (ppb) in the non-living coral sample. $^{232}Th_{live}$ is the mean measured ^{232}Th value (ppb) determined to be 0.95 ppb and $^{230}Th/^{232}Th_{live}$ represents or approximates the isotopic composition of the hydrogenous component in the dead coral skeleton with an atomic value of $5.85 \times 10^{-6} \pm 20\%$ (which corresponds to an activity value of 1.08 ± 20%) based on live *Porites* corals collected from the Palm Islands region (Clark et al. 2014b) which is of a similar setting to Stone Island. $^{230}Th/^{232}Th_{sed}$ is the detrital component represented by a mean atomic value of $3.53 \times 10^{-6} \pm 20\%$ (which corresponds to an activity value of 0.61 ± 20%) from isochron derived initial $^{230}Th/^{232}Th$ values obtained from dead *Porites* coral skeletons collected from the Palm Islands region (Clark et al. 2014b).

4.1.3 Reef development at SI-S

U-Th ages obtained from coral clasts in the percussion cores collected across the reef flat at SI-S were between 7,247 and 4,324 yBP, indicating that most of the reef was constructed during this period (Fig. 3A). Reef initiation occurred prior to 7,247 yBP, as indicated by the U-Th age at the base of S-PC6 4.6 m below the present reef flat surface. Basal ages of ~7,000 yBP were established for S-PC1, S-PC5 and S-PC6. Initial reef development was detached ~330 m seaward of the contemporary shoreline (Fig. 3A), and vertical reef accretion occurred in two parallel, detached parts of the reef. Average vertical reef growth rates during initial stages of reef development were 3.0 mm/yr, which increased to 4.4–4.8 mm/yr between 7,000–6,000 yBP (Fig. 3A). The fossil microatoll age of 6,716 yBP on the SI-S transect confirms that reef flat development at sea level had begun by this time ~200 m offshore from the modern beach. Emplacement of the entire reef flat took ~1,000 years, as indicated by mid-Holocene aged fossil microatolls that occur across the breadth of the reef flat: 6,683 yBP close to the shoreline and 5,894 yBP at the contemporary reef edge (Fig. 3A). Negligible reef progradation has occurred since this time.

Table 2. Core facies descriptions and matrix components including percent sand, mud and carbonate ($CaCO_3$) content (mean and 1σ standard deviation [SD]).

Facies			**A**		**B**		**C**		**D**
Facies name			Contemporary intertidal sands		Reef framework, sandy matrix		Reef framework, muddy-sand matrix		Reef framework, mud matrix
Description			Sandy matrix with encrusted coral rubble and shell hash. Coral clasts are matrix-supported.		Sandy matrix with coral clasts (mainly detrital and matrix-supported), shell hash and bivalves.		Muddy-sand matrix with coral clasts (mainly clast-supported), bivalves and shell hash.		Muddy matrix dominated by coral clasts (mainly clast-supported) with some shell hash.
Environmental interpretation			Contemporary intertidal reef flat.		Lower intertidal reef flat environment where most fine material remains in suspension.		Shallow subtidal reef environment where fine sediments can settle.		Subtidal reef slope where fine sediments can settle.
Matrix component	**Location**		SI-S	SI-N	SI-S	SI-N	SI-S	SI-N	SI-S*
	% sand	Mean	95.8	90.4	91.4	86.5	64.1	79.3	52.2
		SD	2.0	5.2	4.4	7.0	12.7	5.3	13.9
	% mud	Mean	4.2	9.6	8.6	13.5	35.9	20.7	47.8
		SD	2.0	5.2	4.4	7.0	12.7	5.3	13.9
	% $CaCO_3$	Mean	96.9	92.7	91.7	87.4	75.4	81.7	70.5
		SD	2.3	2.8	8.8	6.0	7.9	9.7	9.5

*Facies D only recovered in cores from SI-S.

4.1.4 Reef development at SI-N

Reef development in Shoalwater Bay (SI-N) began prior to 7,064 yBP, as indicated by the U-Th age in N-PC5 4.6 m below the present reef flat surface and ~30 cm above the base of the core (Fig. 3B). After initiation, the reef accreted vertically towards sea level and the oldest fossil microatoll age on the reef flat surface shows that reef flat formation had begun by 4,475 yBP (Fig. 3B). Vertical reef growth rates were generally slower between 7,000–4,300 yBP compared to SI-S, ranging from 0.9–1.7 mm/yr, however there were periods when average rates of reef growth were higher (5.0 mm/yr between 6,812–6,718 yBP documented in N-PC2, Fig. 3B). The majority of the reef flat was emplaced by around 4,000 yBP. Fossil microatoll ages at the outer reef flat of 2,091 yBP and 2,018 yBP indicate that limited reef flat accretion has occurred over the past two millennia (Fig. 3B).

4.2 Contemporary eco-geomorphology

Eco-geomorphological zones were differentiated across the reef transects based on the benthic surveys (Table 3, Fig. 4). The number of zones differentiated varied between sites. Eight zones were differentiated across the transect at SI-S, seven zones across the transect at SI-N, six zones across transect MI-1, and eight zones across transect MI-2 at Middle Island. Generally, the backreef flat environment at all reefs extended from the shoreline at an elevation ~1.0 mLAT (Fig. 3, 5). Each reef flat gently sloped seaward from the backreef flat towards the reef crest, which was elevated close to LAT level at Middle Island (Fig. 5), and below LAT at Stone Island (~0.8 and 0.2 m below LAT at SI-S and SI-N, respectively, Fig. 3). Transitions between zones were subtle in most cases, however a distinctive benthic composition and surface elevation depicted each zone. At all sites the backreef flat was comprised of sand, coral rubble and macroalgae, however live coral cover on the outer reef flat was highly variable between sites.

4.2.1 The fringing reef at SI-S

The elevated backreef flat extended ~130 m from the shoreline and comprises zones 1 and 2 (Fig. 3A), which were characterised by rippled sands (63.0 ± 19.9 and 48.1 ± 13.4% sand cover in zones 1 and 2, respectively) with sparse, patchy macroalgae cover (9.6 ± 15.8 and 39.3 ± 20.3% macroalgae cover in zones 1 and 2, respectively). At the end of zone 2, the reef flat abruptly transitioned to zone 3, where the cemented reef pavement was largely covered with turf algae, along with patchy sand cover (20.0 ± 19.7%) and coral rubble (18.5 ± 7.7%). The outer ~160 m of the reef flat comprises zones 4 and 5, which were both characterised by a sand and coral rubble substrate, dominated by macroalgae (53.3 ± 22.6 and 67.1 ± 22.3% macroalgae cover in zones 4 and 5, respectively). Three key macroalgae genera were identified at SI-S (*Padina*, *Sargassum* and *Halimeda*), however several other unidentified genera were encountered.

Fossil microatolls, mostly *Porites*, were common in all zones across the reef flat. The fossil microatolls across the backreef flat (zones 1 and 2) were generally smaller (1.0–2.8 m in diameter) with upper surfaces at higher elevations (1.0–1.2 mLAT) than those on the outer reef flat (zones 3–5), which tended to be larger (1.5–4.7 m in diameter) with upper surfaces elevated between 0.1–0.6 mLAT. Fossil microatolls across the SI-S reef flat varied in age from 7,103 to 3,787 yBP (Table 1).

The narrow reef slope at SI-S began at the end of zone 5 ~400 m offshore at an elevation ~0.8 m below LAT (Fig. 3A). The reef slope was characterised by a sand and coral rubble substrate, dominated by macroalgae (largely *Sargassum*, Fig. 4). Macroalgae cover on the upper reef slope (zone 6) averaged 51.1 ± 28.6%. A narrow 20 m wide live coral zone (zone

7) extended across the reef slope at a depth ~1.9–2.5 m below LAT (Fig. 3A, Fig. 4). Here, the substrate was sandy (38.5 ± 41.8% cover) with sparse macroalgae cover (17.0 ± 21.2%). Live coral cover was 33.3 ± 21.1%. Mature branching and plate *Acropora* dominated (accounting for 67% of the live corals), but massive corals (genus un-identified) also occurred. Macroalgae cover on the lower reef slope (zone 8) averaged 24.7 ± 28.3%, with no live corals on the slope below -2.5 mLAT depth. Beyond the end of the reef slope at 3.4 m below LAT, a muddy-sand substrate was encountered.

4.2.2 The fringing reef at SI-N

The elevated backreef flat environment, extending ~220 m from the shore, was partly covered by two discrete patches of sand that were almost entirely rippled sand and/or muddy-sand (zones 2 and 4, Fig. 4). These sand areas were generally elevated ~1.0–1.3 mLAT (Fig. 3B). The reef flat surface that was buried by the sand deposits was exposed at zone 3 at ~0.8 mLAT and was largely sandy (66.3 ± 30.8% cover) with sparse coral rubble and macroalgae (Fig. 3B). The outer ~240 m of the reef flat (zone 5) was dominated by macroalgae (*Padina* and *Sargassum*) which averaged 60.9 ± 26.4% of the benthic cover (Fig. 3B) and was found to be at a lower elevation (ranging from 0.7 m above LAT to 0.2 m below LAT). Live corals were sparsely distributed across the outer half of zone 5 (though these were not included in the benthic survey as they were not captured by the random sampling strategy). Two open-water live *Porites* microatolls located inn zone 5 had upper living rims elevated at 0.4 and 0.5 mLAT (one of the microatolls was 2.9 m in diameter; the other ~0.7 m). Fossil *Porites* microatolls were also surveyed across the reef and varied from 1.0–5.5 m in diameter with upper surfaces elevated 0.6–0.8 mLAT. The age of these fossil microatolls at SI-N varied from 4,475–2,018 yBP (Table 1).

Zone 5 terminated ~400 m offshore and ~0.2 m below LAT, beyond which a subtle transition from the reef flat to the narrow reef slope occurred. The reef slope at SI-N was characterised by living corals, coral rubble and sand (Fig. 4, Electronic Supplementary Materials 1). The upper reef slope (zone 6) extended to a depth ~1.8 m below LAT, and live coral cover was high (46.0 ± 36.2% and maximum 96.3% live coral cover). The lower reef slope (zone 7) extended from 1.8–3.2 m below LAT and here, the substrate was dominated by coral rubble (75.7 ± 23.4% cover); live coral cover averaged 18.5 ± 23.7%. Across the reef slope, the dominant coral morphologies were branching (accounting for 32% and 63% of live corals in zone 6 and 7, respectively) and encrusting corals such as *Acropora* and *Montipora* (33% of live corals in zone 6), followed by plate corals of *Acropora* (24% of live corals in zone 6). Columnar, foliaceous, free-living and massive corals were also encountered on the surveys but were uncommon (<5% of the live corals in zone 6). The reef slope ended ~3.2 m below LAT, beyond which the seafloor comprised rippled muddy sands.

4.2.3 Fringing reef at Middle Island

The higher elevation backreef flat at Middle Island (zones 1 and 2) extended 180–220 m offshore, and mainly comprised sand, rubble and macroalgae (34.5 ± 15.4% on MI-1 and included *Padina*, *Sargassum* and *Halimeda*). Fossil microatolls (mainly *Porites*) varying between 1.0–5.3 m in diameter and with upper surfaces elevated between 0.9–1.4 mLAT were scattered throughout zones 1 and 2. Most of the fossil microatolls sampled at Middle Island were much younger than at Stone Island (Fig. 5, Ryan et al. 2016b), ranging from 240 ± 5 yBP to 78 ± 8 yBP. A single mid-Holocene aged fossil microatoll at the backreef dating to 6,895 yBP was the only exception. Open-water live corals occurred on the backreef flat at elevations below 0.8 mLAT, but they were more abundant on the lower elevation MI-1 (21.0 ± 28.7% cover in zone 2) than MI-2 (5.3 ± 7.7% cover in zone 2) (Table 3). Live coral cover was highest (27.0 ± 32.3 to 63.1 ± 20.2%) on the outer parts of the reef flat <0.6 mLAT (zones 3 and 4 on MI-1, and zone 3 on MI-2, Fig. 5). Live hard corals from six genera were recorded across the reef flat: branching *Acropora*, *Montipora* and *Pocillipora*, and massive *Goniastrea*, *Porites*, and *Dipsastraea*. Soft corals were also surveyed, including *Lobophytum*, *Sinularia* and *Sarcophyton*. Branching corals of *Montipora* and *Acropora* were dominant (71% and 92% of live corals in zone 3 on MI-1 and MI-2, respectively).

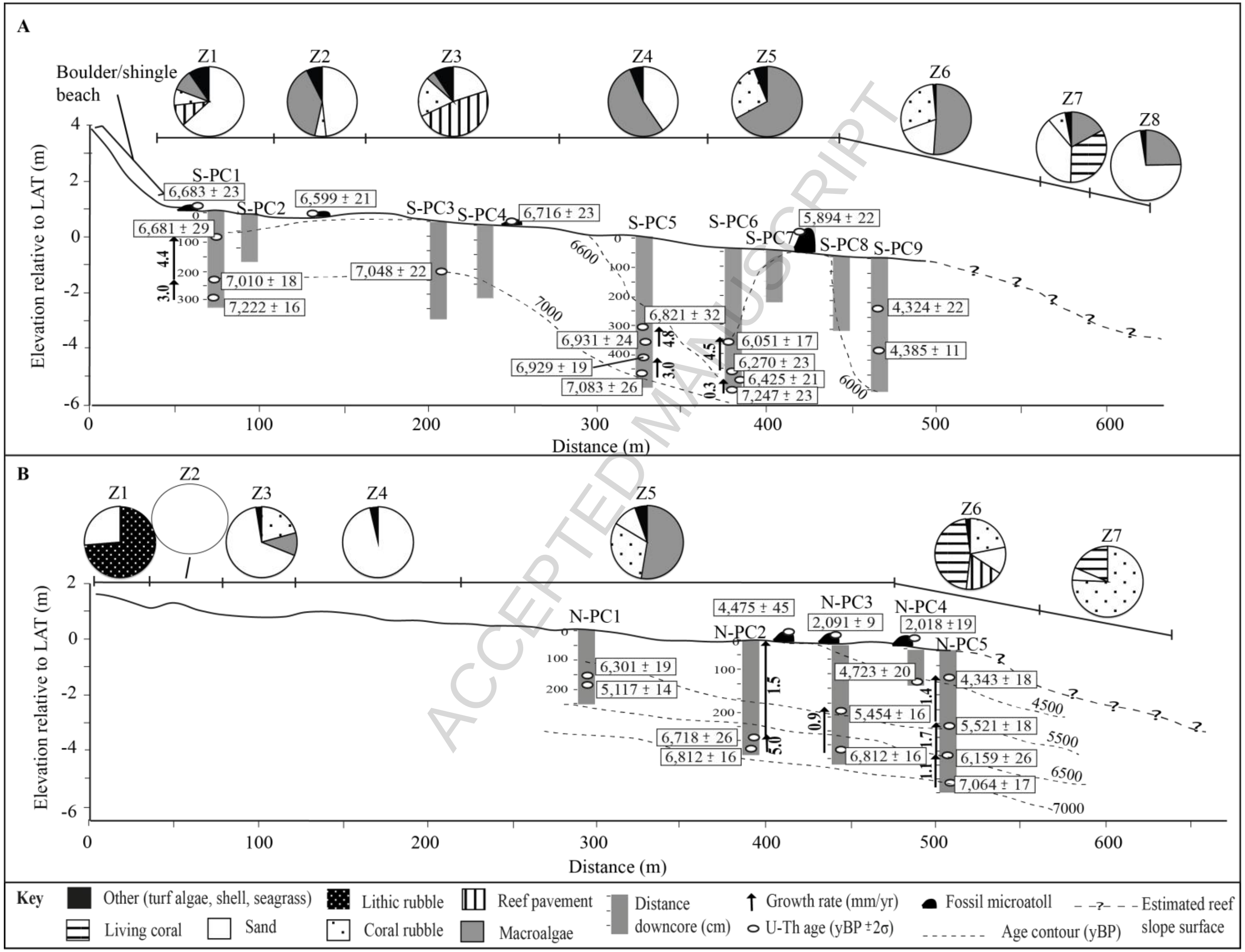

Fig. 3. Profiles of the reef at (A) SI-S and (B) SI-N extending seaward, with reef age indicated by the U-Th ages on the fossil microatolls and in the percussion cores (labelled grey rectangles). The arrows indicate average vertical accretion rates (mm/yr). Elevation is relative to lowest astronomical tide (LAT). Benthic composition of each contemporary eco-geomorphological zone (numbered Z1–8) indicated by shaded pie charts.

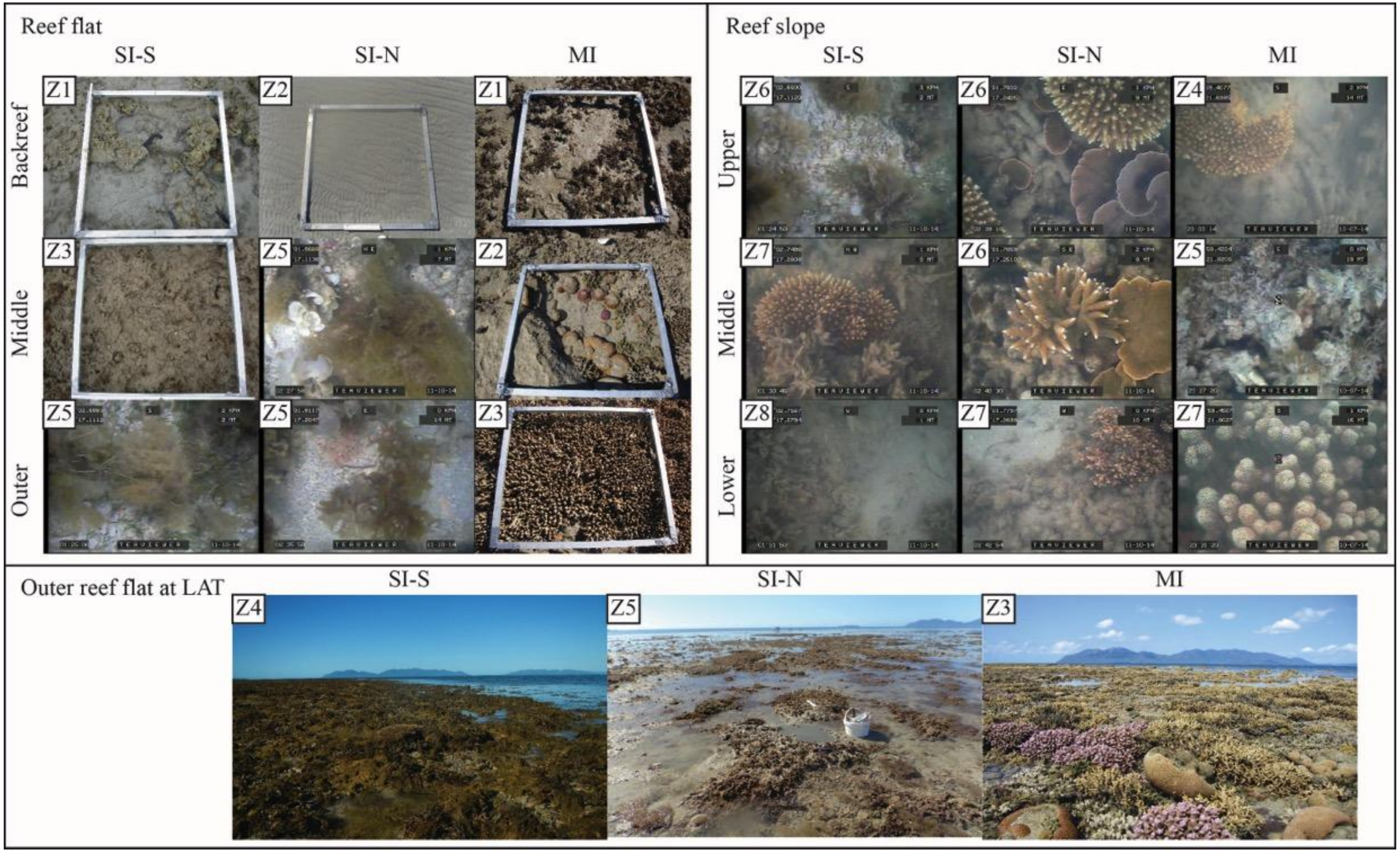

Fig. 4. Upper photographs are from the quadrat and drop camera surveys, illustrating the differences in benthic cover across the reef at Stone Island South (SI-S), Stone Island North (SI-N) and Middle Island (MI). Note sand and macroalgae dominance on the reef flat at SI-S and SI-N, SI-S Z6 and Z8, MI Z1 and Z5. Note live coral cover shown in photographs, including: massive *Porites* (MI Z2); *Goniastrea* (MI Z2); branching or plate *Acropora* (MI Z3 and Z4, SI-N Z6, SI-S Z7); branching *Montipora* (MI Z3); encrusting and foliaceous corals (SI-N Z6); columnar coral (MI Z7). Lower photographs are of the outer reef flat at lowest astronomical tide (LAT). Note macroalgal dominance at SI-S and SI-N and coral dominance (branching *Acropora*, massive Faviids) at MI. Eco-geomorphological zone numbers indicated in top left corner of each photograph. See Electronic Supplementary Materials 1 for elevations of the reef flat surface.

Different ecological zones were identified across the reef slope (Fig. 4, Fig. 5). The upper reef slope was dominated by macroalgae (89.6 ± 15.8% in zone 5 at MI-1) including *Sargassum*, *Turbinaria ornata*, *Padina*, *Chnoospora* and several un-identified genera. Macroalgae mostly grew upon/amongst branching coral rubble. Live coral cover was highest on the lower slopes, particularly on MI-2 in zone 7, which was completely covered by monospecific stands of *Goniopora* and *Galaxea* (100 ± 0.0% coral cover). Other areas of the lower slope contained 13.3 ± 24.1 to 17.3 ± 18.6% live coral cover, where encrusting and foliaceous corals were dominant on MI-1 in zone 6 (including *Leptoseris* and *Galaxea*). A featureless muddy-sand substrate extended beyond the end of the reef slope.

5. Discussion

Comparisons of historical and contemporary photographs of the Stone Island reef flat (Wachenfeld, 1997) have shown a decline in coral cover and structural diversity between 1883 and 1994. These changes have been interpreted as an ecological phase-shift from a coral-dominated to macroalgae-dominated reef flat and have been used as evidence of the broader decline of inshore reefs on the GBR (Hughes et al. 2010; GBRMPA, 2014). This conclusion was reached without consideration of a) documented changes in reef condition between the two photographed periods; b) the longer (millennial-scale) record of reef growth preserved in the reef structure; and c) the condition of other coral reefs within Edgecumbe Bay. Our data from Stone Island provide information and context over multiple timescales to allow for a more comprehensive interpretation of the photographic records of reef condition. The Holocene reef chronostratigraphies established from Stone Island provide baseline long-term data about underlying reef geomorphic state, which combined with other historically documented changes, are valuable for interpreting recently observed variations and changes in reef condition. Coupled with photographic and other evidence, the benthic survey data show that the reef at SI-S had less hard coral cover and more macroalgae

Table 3. Details of contemporary eco-morphological zones at Stone Island and Middle Island. Elevation is relative to lowest astronomical tide (LAT).

Site	Zone	Description	Width (m)	Approximate elevation relative to LAT (m)	Average live coral cover (% mean ± 1 sd)	Notes	Coral genera present (order of dominance)
Stone Island South	1	Sandy backreef flat	70	1.0–0.7	0	Fossil *Porites* microatolls	
	2	Sandy backreef flat with high macroalgae cover	57	0.9–0.7	0	Fossil *Porites* microatolls	
	3	Cemented reef pavement, sand and rubble	112	0.9–0.3	0	Fossil *Porites* microatolls	
	4	Sandy intertidal outer reef flat largely covered in macroalgae	85	0.3 to -0.2	0	Fossil *Porites* microatolls	
	5	Subtidal outer reef flat dominated by macroalgae	76	-0.2 to -0.8	0	Fossil *Porites* microatolls	
	6	Upper reef slope with sand, macroalgae and rubble	114	-0.8 to -1.9	0		
	7	Living coral zone on reef slope with macroalgae	20	-1.9 to -2.5	33.3 ± 21.1	Branching and massive corals dominant	*Acropora*, *Pocillopora*, unidentified massive corals with meandering corallites
	8	Lower reef slope with sand and sparse macroalgae	26	-2.5 to -3.4	0		
Stone Island North	1	Terrigenous rocks and sand	24	1.6–1.0	0		
	2	Muddy-sand flat covering backreef flat	56	1.3–0.9	0		
	3	Backreef flat dominated by sand and rubble with sparse macroalgae	52	0.8	0		
	4	Sand flat covering old reef flat	112	1.0–0.6	0		
	5	Sandy outer reef flat dominated by macroalgae	240	0.7 to -0.2	0	Fossil and live *Porites* microatolls	*Porites*
	6	Upper reef slope live coral zone	50	-0.2 to -1.8	46.0 ± 36.2	Encrusting and branching corals dominant	*Acropora, Montipora, Turbinaria, Favites, Fungia*, Soft corals
	7	Lower reef slope live coral and rubble zone	85	-1.8 to -3.2	18.5 ± 23.7	Branching corals dominant	*Acropora, Montipora, Pocillopora, Platygyra, Fungia*
Middle Island Transect 1	1	Sandy back reef flat with macroalgae and rubble	90	1.0–0.8	0		
	2	Reef flat zone with live corals and fossil microatolls	90	0.8–0.7	21.0 ± 28.7	Branching corals dominant	*Montipora, Goniastrea, Porites*
	3	Reef flat live coral zone	75	0.7–0.6	47.5 ± 28.2	Fossil *Porites* microatolls, branching corals dominant	*Montipora*, Soft corals, *Goniastrea, Acropora, Porites, Pocillopora*
	4	Reef flat edge live coral zone with rubble	75	0.5–0	27.0 ± 32.3	Branching and massive corals dominant	*Acropora, Dipsastraea, Goniastrea*, Soft corals, *Porites, Pocillopora*
	5	Upper reef slope, macroalgae dominated	64	?	2.0 ± 5.6	Macroalgae covering branching coral rubble	*Acropora*
	6	Sandy lower reef slope, live coral zone	47	?	13.3 ± 24.1	Encrusting and foliaceous corals dominant	*Leptoseris, Galaxea*

Middle Island Transect 2	1	Sandy backreef flat dominated by rubble	150	1.0	0.2 ± 0.6	Fossil and live *Porites* microatolls (moated)	*Porites* (moated), *Montipora* (moated)
	2	Sand and rubble zone on reef flat	70	1.0–0.6	5.3 ± 7.7	Branching corals dominant	*Montipora, Goniastrea*
	3	Live coral zone on reef flat	100	0.6–0	63.1 ± 20.2	Branching corals dominant	*Montipora, Acropora, Goniastrea*
	4	Reef crest/upper slope	38	~0	22.9 ± 31.3	Branching corals dominant	*Acropora, Platygyra,* Soft corals
	5	Upper/mid reef slope macroalgae zone	74	?	4.1 ± 9.7	Macroalgae covering branching coral rubble	Unidentified encrusting corals
	6	Mid-reef slope live coral zone	14	?	43.7 ± 42.0	Branching corals dominant	*Acropora,* Soft corals, unidentified massive coral, *Galaxea*
	7	Lower slope live coral zone	23	?	100.0 ± 0.0	Widespread massive coral colonies	*Goniopora, Galaxea*
	8	Sandy lower slope	19	?	17.3 ± 18.6		*Galaxea,* unidentified foliaceous coral

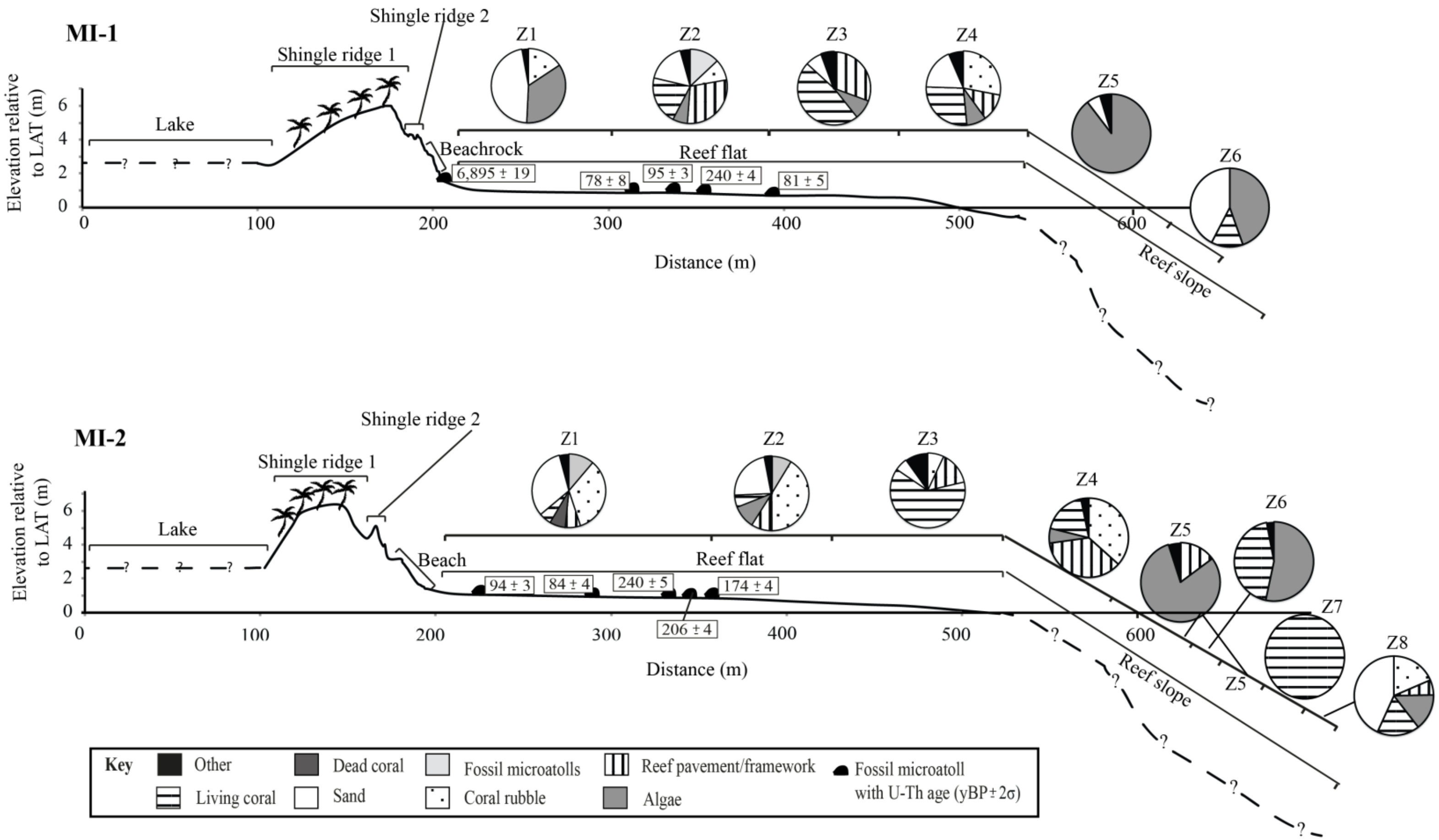

Fig. 5. Profiles of transects MI-1 and MI-2 at Middle Island extending seaward where elevation is relative to lowest astronomical tide (LAT). Benthic composition of each eco-geomorphological zone (numbered Z1–Z8) is indicated by the shaded pie charts. Note that depth of slope is roughly estimated. The fossil microatoll ages are from Ryan et al. (2016b).

than the reef at SI-N and there is nowhere on either reef flat at Stone Island that is comparable to the reef flat condition shown in the photographs presented by Saville-Kent (1893). To better understand the drivers of this change, we first discuss our findings from Stone Island in the context of different temporal scales and consider the timing and extent of ecological change. Second, we investigate the extent of the present reef condition at SI-S across local and regional scales by comparing our findings from Stone Island with other fringing reef flats in Edgecumbe Bay. Collectively, the comprehensive temporal and spatial datasets on the variability in reef condition across Edgecumbe Bay allow for the examination of reef recovery timeframes and an evaluation of the prospects of recovery at Stone Island.

5.1 Stone Island reef – temporal variability

5.1.1. Early-mid Holocene reef development (millennial scale)

Coral colonies established at both Stone Island reefs prior to 7,000 yBP (Fig. 3). Although the percussion cores collected at Stone Island did not penetrate to pre-reefal substrates, it is likely that coral colonies established in a subtidal setting, upon similar substrates to those elsewhere in Edgecumbe Bay. Core records have shown that Middle Island reef initiated about the same time as the Stone Island reefs (~7,800 yBP) directly upon weathered regolith (Ryan et al. 2016b) and Bramston Reef, located ~2 km south-west of Stone Island, developed upon terrigenous transgressionary sands and lag gravels overlying Pleistocene clay (Ryan et al. 2016a). However, the shallower substrate at Bramston Reef was first colonised ~2,000 years after reef initiation at Stone Island (Ryan et al. 2016a).

After initiation, each reef at Stone Island developed in a different way, resulting in distinct modes/styles of growth: episodic reef progradation (Kennedy and Woodroffe, 2002) at SI-S and 'up and out' at SI-N. This resulted in reef flat formation ~2,000 years earlier at SI-S, despite similar timing of reef initiation at both locations. At SI-S, between ~7,200–6,000 yBP the landward part of the reef rapidly accreted vertically towards sea level (up to 4.8 mm/yr on average) at a similar time and pace as a seaward detached, parallel reef (Fig. 3A). The reef first reached sea level at ~6,700 yBP. Subsequently, reef flat formation occurred by landward and seaward progradation of the detached reef sections. The spaces intervening the initially detached reef sections were infilled by a combination of *in situ* reef growth and detrital reef-derived coral rubble material. The majority of the reef flat was emplaced within 1,000 years (by 5,800 yBP). The age structure of the SI-S reef presented here showing episodic reef progradation (Fig. 3A) is largely dependent on the age of a fossil microatoll at the seaward edge of the reef flat (5,894 ± 22 yBP); re-evaluation of our interpretation may be required if potential issues with the age of the fossil microatoll, such as diagenesis have produced an age that may be considered too old. Alternatively, the isochrons may represent a local topographic irregularity in the reef structure (Webb et al. 2016). However, these possibilities are considered unlikely because additional fossil microatolls at the seaward edge alongshore from the transect location at SI-S were also comparatively old, dated at 6,777 ± 20 and 7,103 ± 40 yBP (Figure 3.2 and Appendix 2). Furthermore, the growth mode inferred in the present study conforms to an early reef growth model proposed by Chappell et al. (1983), in which the majority of reef establishment occurred by 6,000 yBP, followed by secondary infilling. Chappell et al. (1983) based this model on the pattern of radiocarbon ages of fossil microatolls (dating to 6,800–6,000 calibrated yBP) across the width of the reef flat at Stone Island, which are similar to the ages obtained in this study: 6,683 yBP at the backreef flat, and 5,894 yBP at the reef flat edge (Fig. 3A). Other fringing reefs where detached reef coalescence has been documented (Kennedy and Woodroffe, 2002) include those at Hayman Island (Hopley et al. 1983; Kan et al. 1997), located ~60 km east of Stone Island, and Yam Island (Woodroffe et al. 2000) in the Torres Strait.

After initiation at SI-N, the reef accreted vertically towards sea level and the majority of the reef structure was developed between ~7,000–4,500 yBP. Once vertical accommodation space was restricted by the defining sea level, reef flat seaward progradation occurred, about 2,000 years after reef flat formation at SI-S. Vertical reef accretion rates were slower at SI-N (0.9–1.7 mm/yr) compared to SI-S (3.0–4.8 mm/yr, Fig. 3), which may be partly attributed to the lower terrigenous mud content in the cores (less than half that compared to SI-S in the lower mud-dominated sediment facies, Table 2). Mud deposition is indicative of low export rates and may enhance reef accretion rates by preserving reef framework material (Perry et al. 2012). Furthermore, the relatively exposed location of SI-N may mean this reef is more subjected to higher frequency disturbances and higher export rates, which would result in lower net reef accretion rates. The 'up and out' mode of reef growth displayed in the reef chronostratigraphy at SI-N is typical of inshore fringing reefs in island embayment settings, such as Pioneer Bay at Orpheus Island, central GBR (Hopley et al. 1983).

5.1.2. Late Holocene (millennial scale)

The majority of both reef structures at SI-N and SI-S have been in place for at least ~4,000 years, when reef accretion slowed or 'turned off' (*sensu* Buddemeier and Hopley, 1988), despite the reefs developing under different modes of growth. At SI-S, the reef developed and achieved high accretion rates under constantly muddy conditions during the mid-Holocene. While the reef crest has not prograded significantly since ~4,000 yBP, it is possible that the subtidal reef slope may have continued to prograde, although at a reduced pace, and has not reached sea level to form a reef flat as in the mid-Holocene (Fig. 3A). After 4,000 yBP reef growth was probably limited to a veneer of living coral at the outer edge of the reef, which is common for inshore GBR reefs of mid-Holocene age (Smithers et al. 2006). No reef material younger than 4,324 yBP at SI-S was dated, likely due to our targeted sampling strategy and/or because material has been moved away by storms/cyclones. We note that material younger than 4,000 yBP has been dated on the SI-S reef flat by Clark et al. (2016). The effects of storms and cyclones on reef growth are evident at Middle Island, where significant quantities of reef material were removed from the reef structure during cyclones in the mid-Holocene and deposited onshore as shingle ridges (Ryan et al. 2016b, Fig. 5). The potential for such storm activity at Stone Island is indicated by storm-deposited beach ridges on the shoreline in Shoalwater Bay and along the south-eastern side of the island, first documented by Hopley (1975). Interestingly, cyclone stripping of the upper outer reef flat at Middle Island between 6,500–1,500 yBP created vertical accommodation space for subsequent reef growth, meaning that the upper ~1.2 m of reef structure is relatively young, having developed since ~1,500 yBP upon the stripped reef surface that initially developed during the mid-Holocene ~6,000 yBP (Ryan et al. 2016b).

Although reef accretion slowed or ceased around 4,000 yBP at SI-N, reef accretion may have 'turned on' (*sensu* Buddemeier and Hopley, 1988) again around 2,000 yBP, as indicated by the fossil microatoll ages of 2,091 yBP and 2,018 yBP at the outer reef flat. A similar turn-off and/or hiatus in active reef accretion between ~4,000–2,000 yBP to that observed at Stone Island has been detected in many reefs of the inshore GBR (Smithers et al. 2006; Perry et al. 2011), including Bramston Reef in Edgecumbe Bay (Ryan et al. 2016a). The causes of this regional hiatus are not completely clear but likely include one or a combination of the following factors: accommodation space constraints caused by late-Holocene sea-level fall (Smithers et al. 2006; Perry et al. 2011); shifts in mid-Holocene sea-surface temperature or climate (Gagan et al. 1998; Roche et al. 2014); and/or terrigenous mud deposition events (Ryan et al. 2016a). Notably, the deceleration in active reef accretion at Stone Island occurred well before European settlement of the coast and was thus driven by natural factors. Indeed, the most productive time for active reef accretion at Stone Island fringing reefs was ~7,000–4,000 years ago. Negligible reef accretion occurred at Stone Island after this, despite regional conditions being suitable for reef accretion between 4,000–1,000 yBP, as indicated by the continued progradation of nearby Bramston Reef during this time (with the exception of a hiatus ~3,000–2,000 yBP, Ryan et al. 2016a).

5.1.3 Contemporary reef condition (centennial-scale to present)

Surveys of contemporary ecological benthic cover confirm that neither reef flat at Stone Island currently supports coral cover comparable with that depicted in Saville-Kent's (1893) photographs, which show a variety of live corals exposed at low water on the reef flat. Rather, the reef flats were dominated by sand, rubble and macroalgae, as shown in the more recent photographs of the reef flat in Wachenfeld (1997) and Clark et al. (2016) taken in 1994 and 2012, respectively and in accord with benthic surveys conducted by Clark et al. (2016) where live coral cover at the SI-S reef flat was 0.09 ± 0.12%. At SI-S macroalgae was more abundant, comprising >50% cover in three zones at SI-S and just one zone at SI-N (Fig. 3). Live coral cover on the reef slope was high at SI-N comprising 46.0 ± 36.2% cover (Table 3, Electronic Supplementary Materials 1). Here, live coral occurred across the upper to lower slope, while on the SI-S reef slope, live coral was restricted to a narrow 20 m zone that also contained macroalgae (Table 3, Fig. 4). In addition, live coral diversity was higher at SI-N with eight hard coral genera identified (*Acropora, Montipora, Turbinaria, Favites, Fungia, Pocillopora, Porites* and *Platygyra*) compared with three identified genera (*Acropora, Porites* and *Pocillopora*) at SI-S (Table 3). Ideally, a comparison of the palaeo-ecological diversity in the long-term percussion core records with the present reef slope diversity would be valuable. However, differentiating coral genera in the video footage was often impossible due to turbidity and thus the eight coral genera identified at SI-N are probably an underestimate of the true generic diversity at this site. Furthermore, the palaeo-ecological data are largely derived from subtidal reef slope environments, which cannot be directly compared to the intertidal reef flat data (benthic surveys, reef flat photographs) due to differences in environmental conditions resulting in naturally different coral assemblages (Chappell, 1980). Videography was a suitable technique in this study for simply quantifying benthic cover, but a more detailed study on reef slope coral cover and diversity at these inshore reefs is needed.

Our study has provided insight to address some of the issues with comparing photographs taken at different times of the Stone Island reef flat alone to make conclusions about regional reef condition. The critical issues are: 1) the exact location of the Stone Island photographs from the late 1800s; 2) the elevation of the reef flat shown in historical and contemporary photographs; and 3) the significance of any documented changes in the context of a longer-term Holocene reef growth history. The location of Saville-Kent's (1893) photographs was indicated by Hedley (1925), which conforms to the landforms in the horizon of several photographs. However, the exact location of Saville-Kent's photographs is unknown, and thus so too is the elevation of the reef flat and corals shown in the photographs. Accurate elevation data of the reef flat surface where historical and recent photographs were taken must be obtained to ensure the possible influence of emergence of the mid-Holocene aged reef flat can be determined. However, elevation is unknown for all existing photographs from Stone Island, except very recent photographs presented in Clark et al. (2016). The tops of the corals in the historical photographs that were taken during spring low tide by Saville-Kent (1893) must have been elevated approximately 0.5–0.3 m above LAT based on our surveys of uppermost open-water coral growth elevation within Edgecumbe Bay. If these photographs were of the outer reef flat (which is now ~0.2–0.8 m below LAT) it is implied that a significant amount of reef material from the outer reef flat has been eroded or scoured away since the photo was taken, as suggested by Clark et al. (2016). Dated fossil microatolls aged between 6,716–5,894 yBP indicate that the entire part of the reef flat at SI-S that is presently exposed at low water developed during the early- to mid-Holocene (Fig. 3a) when sea level was 1.0–1.5 m higher than present (Chappell et al. 1983; Lewis et al. 2013). Thus, much of the backreef flat surface is elevated ~1.0 mLAT, too high for modern open-water live coral growth on the reef flat, which at Middle Island was restricted to below 0.8 mLAT (Table 3) and at Bramston Reef to below ~0.4–0.3 mLAT (Ryan et al. 2016a). This finding casts doubt that the location/elevation of some of the recent photographs of Stone Island reef flat are true replicates of Saville-Kent's images, and raises the possibility that they are in fact images of the older, elevated section of the reef flat. For example, the photograph presented in Bell et al. (2014) taken in 1994 reportedly showing the 'nearshore region' (Bell and Elmetri, 1995) is probably of the higher and senescent mid-Holocene backreef because of the distance it is located from the water's edge. It is easy to misinterpret these photographs without an understanding of the Holocene reef growth history, subtle changes in elevation, and the control this has on intertidal coral growth and survival. Regardless of water quality, coral cover and diversity will naturally never be high if the reef flat elevation is too high and emergence is prolonged. Nevertheless, contemporary photographs from the outer reef flat at Stone Island (Fig. 1) still show very little or no live coral cover. Ultimately, conclusions should not be drawn about changes in reef condition based on the historical photographs that are not spatially (and elevationally with respect to the tidal frame) referenced with great precision and accuracy. However, when combined with quantitative data and long-term knowledge of reef development and palaeo-ecology, photographs can provide additional useful evidence of reef condition.

5.2 Local versus regional effect

Contemporary reef benthic composition varied between SI-N and SI-S (Fig. 3), and also varied between other sites in Edgecumbe Bay. The amount of live coral cover and the elevations at which corals survive varies between reefs and these variations are particularly pronounced on the outer reef flat zones. All the fringing reefs in Edgecumbe Bay for which reef growth histories are known began to develop in the early- or mid-Holocene and have not prograded much since

~2,000 yBP. Nevertheless, live coral cover blankets parts of these old reef structures as a thin veneer of growth, including at Middle Island and Bramston Reef at elevations <0.8 mLAT and <0.4 mLAT, respectively (Table 3, Fig. 4, Ryan et al. 2016a, Electronic Supplementary Materials 1). Based on these other locations in Edgecumbe Bay (including one closer to the mainland than Stone Island) it would be expected that live corals could grow at similar elevations (below at least 0.4 mLAT) at the Stone Island reef flats, providing all other requisites for coral growth were met. Yet this was not the case and live coral cover was very poor on the Stone Island reef flats. Coral growth is possible up to 0.5 mLAT at Stone Island as the upper living rims of *Porites* microatolls were elevated 0.5–0.3 mLAT at SI-N and SI-S (Fig. 2). However, some of the living microatolls were partly smothered by macroalgae, which can impede coral settlement and growth (Fabricius, 2005; Foster et al. 2008; Diaz-Pulido et al. 2010). Live coral cover on the outer reef flat at Middle Island (0.6–0.0 mLAT) was 63.1 ± 20.2% (Fig. 4, Fig. 5, Table 3). Middle Island is clearly an example of an inshore fringing reef flat with exceptionally high coral cover, exceeding the average cover quantified for nearshore patch reef flats (~35%: Perry et al. 2009; ~7%: Browne et al. 2010) and inshore fringing reef flats (5–33%: Bull, 1982; 14%: Ryan et al. 2016a) and slopes (30–40%: Thompson et al. 2013). Furthermore, average coral cover between 1985 and 2012 on the central GBR (largely mid-shelf reef slopes) was only around 15–30% (De'ath et al. 2012); well below that established for the reef flat at Middle Island even though reef flats typically have lower coral cover and are more vulnerable to disturbances than reef slopes.

Presently, coral cover varies between reefs in Edgecumbe Bay as it has done over the past ~150 years (Table 5). However, whether shorter-term fluctuations in reef condition occurred in the longer-term records provided by reef cores is uncertain, as most long-term records do not provide age data at adequate resolution to answer such ecological questions (Pandolfi and Kiessling, 2014). Nevertheless, the longer-term records do suggest that reef accretion has stopped and started on millennial scales, independently of anthropogenic impacts (Ryan et al. 2016a, Fig. 3b).

If recent anthropogenic impacts such as increased sediment and nutrient loads to the inshore GBR have contributed to low coral cover at Stone Island, similar effects are not regionally evident within Edgecumbe Bay. Indeed, parts of Bramston Reef today appear similar to the condition photographed and described by Saville-Kent (1893), while the coral growth at Middle Island matches the descriptions by Agassiz (1898) (Table 5, Electronic Supplementary Materials 1). Thus, the condition of the reefs at Stone Island appears to be a local effect. When using high coral cover at Middle Island as an example, it could be argued that the greater distance offshore is advantageous to reef health due to the location away from major river influences. However, the high coral cover at SI-N upper reef slope (46.0 ± 36.2%) clearly demonstrates that healthy reef growth is possible at this inshore site. A long-term understanding of disturbance and recovery regimes is required to investigate the effects of local factors that may have influenced the recovery potential at Stone Island.

The rate at which a reef recovers after a disturbance is influenced by myriad of factors (Connell et al. 1997; Graham et al. 2011; Kittinger et al. 2011) and inshore reefs likely recover at different rates to their offshore, clear water counterparts (Done et al. 2007). Observed rates of recovery on inshore reefs are variable and poorly understood due to a lack of long-term studies. Observed inshore reef recovery rates were >14 years in Jamaica after a hurricane (Hughes and Connell, 1999), while longer recovery periods (over decades to centuries) have been reported in Hawaii, revealing that over long timeframes reefs may maintain resilience to recover from human impacts (Kittinger et al. 2011). Estimated rates of inshore reef recovery vary from 7 years (Johns et al. 2014) to 15 years (Jones and Berkelmans, 2014) after various disturbance types. Clark et al. (2016) estimated the recovery time at Stone Island reef flat (SI-S) to be 40 to 50 years.

The available qualitative and quantitative data for reef condition in Edgecumbe Bay (Table 4, 5) allow for an appreciation of ecological trends despite being punctuated in time. At Middle Island strong coral community recovery must have occurred over the past 40 years since Hopley's (1975) description. The results of Middle Island reef slope benthic cover showing high coral cover on the lower slope (Table 3, Fig. 5) are compatible with De'Vantier et al.'s (1998) description of the ecological condition of Middle Island reef slope in 1994–1995 as top quality on the lower slope, with above average hard coral cover, hard coral richness and diversity, but poor quality on the upper slope, with below average hard coral cover and above average turf algae cover. At Stone Island however, no recovery is apparent over the past 40 years. Anecdotal evidence (oral) and ages from dead *in situ* coral colonies on Stone Island reef (Clark et al. 2016) suggests that coral communities may have been on the way to recovery during the 1970s (Table 5), fifty years after the 1918 cyclone. The potential of the reef to recover may exist, but regular ecological monitoring is required in the future to quantify any changes in reef condition.

Recovery on inshore reefs may be hindered by shorter intervals between disturbances and/or the reduced supply of coral larvae for recolonisation (Done et al. 2007). The high coral cover on sections of the reef at SI-N and other reefs in Edgecumbe Bay implies that no major regional disturbance has affected these sites in the past decade or so. Small coral recruits were present, although rare at Stone Island, indicating that recruitment can still occur at this site (Done et al. 2007, van Woesik et al. 1999). Whether or not the supply/abundance of recruits has changed over time is unknown. However, the low abundance of coral recruits on Stone Island reef flats compared with Bramston Reef (Ryan et al. 2016a) and Middle Island suggests that either settlement or prolonged survival of recruits is impeded. This warrants further investigation, however hydrodynamic processes such as current velocities and direction may influence recruit settlement (van Woesik et al. 1999). The high abundance of macroalgae at SI-S compared with other locations (Fig. 3) may be contributing to the survival and recovery of coral communities (McCook et al. 2001; Fabricius, 2005; Diaz-Pulido et al. 2010). Furthermore, rippled sand areas at

SI-N are probably quite mobile, and coral recruitment would be difficult on these soft or periodically buried substrates.

Table 4. The geomorphic development of reefs in Edgecumbe Bay over millennia based on reef cores. Time is thousands of years before present (k yBP).

	8–7 k yBP	7–6 k yBP	6–5 k yBP	5–4 k yBP	4–3 k yBP	3–2 k yBP	2 k yBP to present	Reference
Bramston Reef			Initiation, vertical accretion	Rapid vertical accretion (rates up to 3.6 mm/yr), reached sea level	Reef flat prograded seaward	Little accretion	Negligible seaward progradation	Ryan et al. (2016a)
Stone Island South	Initiation, vertical accretion	Rapid vertical accretion (rates up to 4.5 mm/yr), reached sea level	Reef flat prograded, lateral accretion	Negligible seaward progradation	No accretion	No accretion	Negligible seaward progradation	This manuscript
Stone Island North	Initiation, vertical accretion	Rapid vertical accretion (rates up to 5.0 mm/yr)	Vertical and lateral accretion (vertical rates up to 1.7 mm/yr)	Vertical and lateral accretion, reached sea level	No accretion	No accretion	Negligible seaward progradation	This manuscript
Middle Island	Initiation, vertical accretion	Rapid vertical accretion (rates up to 7.6 mm/yr), reached sea level and reef flat prograded	Reef lateral accretion and cyclone stripping	Reef lateral accretion and cyclone stripping	No accretion	No accretion	Veneer of vertical (<1.2 m) and lateral growth	Ryan et al. (2016b)

Table 5. Statements of reef condition in Edgecumbe Bay over the past ~150 years derived from various sources.

Reef site in Edgecumbe Bay	Time (year AD)	Statement of reef condition	Source type	Reference
Bramston Reef	c. 1890	Exposed at low tide was "a grand mass of *Porites*… it's exposed, horizontal surface is for the most part dead and eroded…the eroded upper surface has been adopted as a fulcrum of attachment by various coral types that flourish on a higher vertical plane", including *Goniastrea* and *Acropora.* "abundant development…of a luxuriant crop of seaweeds".	Historical photographs and associated descriptions	Saville-Kent (1893, pp. 15)
Bramston Reef	1994	"Large numbers of faviid colonies…the vast majority are dead and those that are alive are comparatively small (<15 cm)…typically covered in algae and/or mud". Living large *Porites* colonies and microatolls with mud and algae on top of the microatolls.	Photographs and descriptions	Wachenfeld (1997, pp. 138)
Bramston Reef	2012	Live coral cover on outer reef flat on average 7.0 ± 4.7%, including *Acropora, Goniastrea, Montipora, Goniopora, Lobophyllia, Favites, Turbinaria, Pocillipora,* and *Dipsastraea.*	Ecological survey	Clark et al. (2016)
Bramston Reef	2014	Live coral cover on outer reef flat on average 13.9 ± 19.2%, including large *Porites* colonies with dead upper surfaces, colonised by a variety of live soft and hard corals and algae. Reef slope contains zones of high coral cover (up to 51.3 ± 19.4% on average) and zones dominated by macroalgae.	Ecological survey	Ryan et al. (2016a)
Stone Island	c. 1890	Extensive hard coral cover on the reef flat exposed at spring low tide, including *Acropora, Montipora, Goniastrea, Turbinaria, Pavona*.	Historical photographs and associated descriptions	Saville-Kent (1893)
Stone Island	c. 1920	No trace of living coral. "This famous, wonderful and immense structure has now completely vanished. Not only has the coral all died, but every vestige of it, except the foundation, has been swept away"	Descriptions	Hedley (1925); Rainford (1925)

Stone Island	1925	Live coral cover recovering, small colonies of *Goniastrea*, *Merulina*, *Turbinaria* and *Fungia* observed. Soft corals flourishing.	Descriptions	Stanley (1928)
Stone Island	1936-1938	Reef flats "dead on their upper surfaces". Recovery negligible.	Descriptions	Steers (1937); Richards (1938)
Stone Island	1953	Negligible recolonisation	Anecdotal evidence from personal communications	Stephenson et al. (1958)
Stone Island	c. 1970s	Healthy reef flat	Anecdotal evidence from local residents	Wachenfeld (1997)
Stone Island	1990	Reef flat surface dominated by coral rubble and macroalgae. No colonies of *Acropora* exposed on the reef flat at spring low tide. Few massive colonies.	Photographs and descriptions	Wachenfeld (1997)
Stone Island	2012	Reef flat dominated by sand and macroalgae. Extremely low coral cover on the reef flat (average 0.09 ± 0.12%). Live *Acropora, Cyphastrea, Pocillipora, Goniastrea, Platygyra, Dipsastraea* observed.	Photographs and ecological survey	GBRMPA (2014); Clark et al. (2016)
Stone Island	2014	Reef flats dominated by sand, coral rubble and macroalgae with very sparse, small live corals. Reef slope at Shoalwater Bay averaged 46.0 ± 36.2 and 18.5 ± 23.7 live coral cover (branching, encrusting, plate, columnar, foliaceous, free-living and massive). Reef slope on southern side of island dominated by macroalgae with narrow zone containing 33.3 ± 21.1% live coral (branching and massive).	Ecological survey	Current manuscript
Middle Island	1896	The outer face of Middle Island's reef flat was "coated with fine heads of corals…becoming less prominent as they tend towards the shallower edge of the flat".	Historical descriptions	Agassiz (1898, pp. 107)
Middle Island	1970s	Reef flat largely dead.	Geomorphological description	Hopley (1975)
Middle Island	1994-1995	Below average hard coral cover and above average turf algae cover on upper slope. Above average hard coral cover, hard coral richness and diversity on the lower slope.	Ecological survey	De'Vantier et al. (1998)
Middle Island	2014	High coral cover on outer parts of the reef flat (63.1 ± 20.2%) and lower parts of the reef slope (17 ± 18.6 to 100 ± 0.0%).	Ecological survey	Current manuscript

Soft rippled sand substrates were also observed (though not surveyed) on the western side of SI-S reef flat near the sand spit. Indeed, the ~400 m long sand spit indicates a large supply of sediment to this part of the island. The sand spit would be mobile under normal and storm conditions and spit migration may also influence the survival of coral recruits in this area of the reef flat (Hopley et al. 1983).

6. Conclusion

We reconstructed Holocene reef development at two fringing reefs at Stone Island to provide baseline, Holocene data on reef geomorphic state as context for assessing contemporary reef condition. The high-precision U-Th ages from the reef cores show that both reefs began to develop in the early-Holocene, prior to ~7,000 yBP. Despite each reef at Stone Island developing according to different modes/styles of growth and under different sedimentary regimes, the majority of reef growth occurred by 4,000 yBP at both sites. The reef flats developed under a higher mid-Holocene sea level, with the backreef flat environment elevated up to a metre above the level of present reef flat formation. The elevation of the reef flat surface influences the contemporary variability in benthic cover across each reef, with the higher elevation backreef flat zones at all reefs dominated by sand, coral rubble and macroalgae. Open-water live coral cover was restricted to the lower elevation outer reef flats. At Stone Island, live coral cover on the outer reef flats was very scarce, while the outer reef flat at Middle Island was characterised by high coral cover reaching as much as 63.1 ± 20.2%.

The reef at SI-S was in a comparatively poor condition relative to other reefs in Edgecumbe Bay and there was nowhere on the reef flats at Stone Island that was comparable to photographs taken in the late 1800s. Thus, we suggest that localised factors are inhibiting reef flat recovery at Stone Island (particularly SI-S). Our results highlight why photographs of reef flats over time that are not spatially referenced should not be solely used to document changes in reef condition, particularly on a regional scale. Interpretations of photographic records should take into account the long-term development of the reef, the elevation of the reef flat where the photos are taken, and the decadal scale ecological trends and recovery rates, if possible. We do not contest that phase-shifts have occurred on some inshore reefs on the GBR, but we recommend further studies on the reefs where it appears phase-shifts have occurred through photographic evidence (Wachenfeld, 1997) or the lack of accretionary corals (e.g. van Woesik et al. 1999) to gain a more comprehensive understanding. Such studies will provide further insights on the ability of inshore reefs to recover from natural and anthropogenic disturbances.

ACKNOWLEDGEMENTS

This work is a contribution to the National Environmental Research Program (NERP) Project 1.3 'Characterising the cumulative impacts of global, regional and local stressors on the present and past biodiversity of the GBR' to Zhao, Smithers, Clark and others. The authors wish to acknowledge funding from the Great Barrier Reef Marine Park Authority (Science for Management Award to Ryan) and the NERP (PhD scholarship to Ryan). We also extend our gratitude to the staff at the Radiogenic Isotope Facility at the University of Queensland, the crew of the Research Vessel James Kirby and dedicated field volunteers (D. Waltrick, D. Thompson, J. Johnson, G. Endo and S. Ballard). Thoughtful reviews by G. Webb, D. Kennedy and 2 anonymous reviewers significantly improved this manuscript.

LITERATURE CITED

Agassiz, A., 1898. A visit to the Great Barrier Reef of Australia in the steamer "Croydon" during April and May, 1896. Bulletin of the Museum of Comparative Zoology, Harvard College. 28, 93-148.

Alvarez-Filip, L., Dulvy, N.K., Cote, I.M., Watkinson, A.R., Gill, J.A., 2011. Coral identity underpins architectural complexity on Caribbean reefs. Ecological Applications. 21(6), 2223-2231.

Andutta, F.P., Ridd, P.V., Wolanski, E., 2013. The age and the flushing time of the Great Barrier Reef waters. Continental Shelf Research. 53, 11-19.

Bartram, G., 1972. The dam that grew…and grew…into a lake. The Australian Women's Weekly. Accessed at http://trove.nla.gov.au/ndp/del/article/51274151?searchTerm=%2522Stone%20Island%2522%20AND%20%2522bowen%2522%20AND%20%2522dam%2522&searchLimits. On 10 February 2016.

Bell, P.R.F., Elmetri, I., 1995. Ecological indicators of large-scale eutrophication in the Great Barrier Reef lagoon. Ambio. 24(4), 208-215.

Bell, P.R.F., Elmetri, I., Lapointe B.E., 2014. Evidence of large-scale chronic eutrophication in the Great Barrier Reef: Quantification of chlorophyll *a* thresholds for sustaining coral reef communities. Ambio. 43(3), 361-376.

Bellwood, D.R., Hughes, T.P., Folke, C., Nystrom, M., 2004. Confronting the coral reef crisis. Nature. 429, 827-833.

Bowen Independent, 1916. Pleasure resorts. Bowen Independent. pp. 2. Accessed at http://trove.nla.gov.au/ndp/del/article/196356917?searchTerm=%22Stone%20Island%22%20AND%20%22goats%22&searchLimits=. On 10 February 2016.

Bowen Independent, 1934. Spitfire survey of Port Denison. Bowen Independent. pp. 1. Accessed at http://trove.nla.gov.au/ndp/del/article/193100480?searchTerm=%22Stone%20Island%22%20AND%20%22sheep%22&searchLimits=. On 10 February 2016.

Brodie, J., Ariel, E., Thomas, C., O'Brien, D., Berry, K., 2014. Links between water quality and marine turtle health, a technical report to the World Wildlife Fund, Centre for Tropical Water & Aquatic Ecosystem Research (TropWATER).

Browne, N.K., Smithers, S.G., Perry, C.T., 2010. Geomorphology and community structure of Middle Reef, central Great Barrier Reef, Australia: an inner-shelf turbid zone reef subject to episodic mortality events. Coral Reefs. 29, 683-689.

Browne, N.K., Smithers, S.G., Perry, C.T., 2012. Coral reefs of the turbid inner-shelf of the Great Barrier Reef, Australia: An environmental and geomorphic perspective on their occurrence, composition and growth. Earth-Science Reviews. 115, 1-20.

Bruno, J.F., Selig, E.R., 2007. Regional decline of coral cover in the Indo-Pacific: timing, extent, and subregional comparisons. PloSOne. 2(8), e711. doi:10.1371/journal.pone.0000711.

Bruno, J.F., Sweatman, H., Precht, W.F., Selig, E.R., Schutte, V.G.W., 2009. Assessing evidence of phase shifts from coral to macroalgal dominance on coral reefs. Ecology. 90(6), 1478-1484.

Budd, A.F., Fukami, H., Smith, N.D. and Knowlton, N., 2012. Taxonomic classification of the reef coral family Mussidae (Cnidaria: Anthozoa: Scleractinia). Zoological Journal of the Linnean Society. 166, 465-529.

Buddemeier, R.W., Hopley, D., 1988. Turn-ons and turn-offs: causes and mechanisms of the initiation and termination of coral reef growth. Proceedings of the Sixth International Coral Reef Symposium, Townsville, Australia. pp. 253-261.

Bull, G.D., 1982. Scleractinian coral communities of two inshore high island fringing reefs at Magnetic Island, North Queensland. Marine Ecology Progress Series. 7, 267-272.

Chappell, J., 1980. Coral morphology, diversity and reef growth. Nature. 286, 249-252.

Chappell, J., Chivas, A., Wallensky, E., Polach, H., Aharon, P., 1983. Holocene palaeo-environmental changes central to north Great Barrier Reef inner zone. BMR Journal of Australian Geology and Geophysics. 8, 223-235.

Cheng, H., Edwards, R.L., Hoff, J., Gallup, C.D., Richards, D.A., Asmerom, Y., 2000. The half-lives of uranium-234 and thorium-230. Chemical Geology. 169, 17-33.

Clark, T.R., Roff, G., Zhao, J., Feng, Y., Done, T.J., Pandolfi, J.M., 2014a. Testing the precision and accuracy of the U-Th chronometer for dating coral mortality events in the last 100 years. Quaternary Geochronology. 23, 35-45.

Clark, T.R., Zhao, J.X., Roff, G., Feng, Y.X., Done, T.J., Nothdurft, L.D., Pandolfi, J.M., 2014b. Discerning the timing and cause of historical mortality events in modern *Porites* from the Great Barrier Reef. Geochimica et Cosmochimica Acta. 138, 57-80.

Clark, T.R., Leonard, N.D., Zhao, J.X., Brodie, J., McCook, L.J., Wachenfeld, D.R., Nguyen, A.D., Markham, H.L., Pandolfi, J.M., 2016. Historical photographs revisited: a case study for dating and characterizing recent loss of coral cover on the inshore Great Barrier Reef. Scientific Reports. 2, DOI: 10.1038/srep19285.

Connell, J.H., Hughes, T.P., Wallace, C.C., 1997. A 30-year study of coral abundance, recruitment, and disturbance at several scales in space and time. Ecological Monographs. 67(4), 461-488.

De'ath, G., Fabricius, K.E., Sweatman, H., Puotinen, M., 2012. The 27-year decline of coral cover on the Great Barrier Reef and its causes. Proceedings of the National Academy of Sciences. 65, 1-5.

DeVantier, L.M., De'ath, G., Done, T.J., Turak, E., 1998. Ecological assessment of a complex natural system: a case study from the Great Barrier Reef. Ecological Applications. 8(2), 480-496.

Diaz-Pulido, G., Harii, S., McCook, L.J., Hoegh-Guldberg, O., 2010. The impact of benthic algae on the settlement of a reef-building coral. Coral Reefs. 29, 203-208.

Done, T., Turak, E., Wakeford, M., DeVantier, L., McDonald, A., Fisk, D., 2007. Decadal changes in turbid-water coral communities at Pandora Reef: loss of resilience or too soon to tell? Coral Reefs. 26, 789-805.

Fabricius, K.E., 2005. Effects of terrestrial runoff on the ecology of corals and coral reefs: review and synthesis. Marine Pollution Bulletin. 50, 125-146.

Fabricius, K.E., De'ath, G., McCook, L., Turak, E., Williams, D.McB., 2005. Changes in algal, coral and fish assemblages along water quality gradients on the inshore Great Barrier Reef. Marine Pollution Bulletin. 51, 384-398.

Foster, N.L., Box, S.J., Mumby, P.J., 2008. Competitive effects of macroalgae on the fecundity of the reef-building coral *Montastraea annularis*. Marine Ecology Progress Series. 367, 143-152.

Gagan, M.K., Ayliffe, L.K., Hopley, D., Cali, J.A., Mortimer, G.E., Chappell, J., McCulloch, M.T., Head, M.J., 1998. Temperature and surface-ocean water balance of the mid-Holocene tropical western Pacific. Science. 279, 1014-1018.

Gardner, T.A., Côté, I.M., Gill, J.A., Grant, A., Watkinson, A.R., 2003. Long-term regional-wide declines in Caribbean corals. Science. 301, 958-960.

Gilmour, J.P., Smith, L.D., Heyward, A.J., Baird, A.H., Pratchett, M.S., 2013. Recovery of an isolated coral reef system following severe disturbance. Science. 340, 69-71.

Great Barrier Reef Marine Park Authority (GBRMPA), 2013. Don basin assessment: Burdekin dry tropics natural resource management section. GBRMPA, Townsville.

Great Barrier Reef Marine Park Authority (GBRMPA), 2014. Great Barrier Reef Outlook Report. GBRMPA, Townsville.

Graham, N.A.J., Nash, K.L., Kool, J.T., 2011. Coral reef recovery dynamics in a changing world. Coral Reefs. 30, 283-294.

Green, D.H., Edmunds, P.J., Carpenter, R.C., 2008. Increasing relative abundance of *Porites astreoides* on Caribbean reefs mediated by an overall decline in coral cover. Marine Ecological Progress Series. 359, 1-10.

Hedley, C., 1925. The natural destruction of a coral reef. Transactions of the Royal Geographical Society of Australasia (Queensland). Reports of the Great Barrier Reef Committee. 1, 35-40.

Hoegh-Guldberg, O., 2014. Coral reefs in the Anthropocene: persistence or the end of the line? In: Waters, C.N., Zalasiewicz, J.A., Williams, M., Ellis, M.A., Snelling, A.M. (Eds.) A stratigraphical basis for the Anthropocene. Geological Society, London. Special Publications. 395, 167-183.

Hopley, D., 1975. Contrasting evidence for Holocene sea levels with special reference to the Bowen-Whitsunday area of Queensland. In: Douglas, I., Hobbs, J.E., Pigram, J.J. (Eds.) Geographical essays in honour of Gilbert J. Butland. University of New England, Armidale, pp. 51-84.

Hopley, D., Slocombe, A.M., Muir, F., Grant, C., 1983. Nearshore fringing reefs in North Queensland. Coral Reefs. 1, 151-160.

Hopley, D., Smithers, S., Parnell, K., 2007. The Geomorphology of the Great Barrier Reef: Development, Diversity and Change. Cambridge University Press, Cambridge.

Hughes, T.P., 1994. Catastrophes, phase shifts, and large-scale degradation of a Caribbean coral reef. Science. 265, 1547-1551.

Hughes, T.P., Connell, J.H., 1999. Multiple stressors on coral reefs: a long-term perspective. Limnology and Oceanography. 44, 932-940.

Hughes, T.P., Graham, N.A.J., Jackson, J.B.C., Mumby, P.J., Steneck, R.S., 2010. Rising to the challenge of sustaining coral reef resilience. Trends in Ecology and Evolution. 25, 633-642.

Hughes, T.P., Bellwood, D.R., Baird, A.H., Brodie, J., Bruno, J.F., Pandolfi, J.M., 2011. Shifting base-lines, declining coral cover, and the erosion of reef resilience: comment on Sweatman et al. (2011). Coral Reefs. 30, 653-660.

Hughes, T.P., Rodrigues, M.J., Bellwood, D.R., Ceccarelli, D., Hoegh-Guldberg, O., McCook, L., Moltschaniwskyj, N., Pratchett, M.S., Steneck, R.S., Willis, B., 2007. Phase shifts, herbivory, and the resilience of coral reefs to climate change. Current Biology. 17, 360-365.

Johns, K.A., Osborne, K.O., Logan, M., 2014. Contrasting rates of coral recovery and reassembly in coral communities on the Great Barrier Reef. Coral Reefs. 33, 553-563.

Jones, A.M., Berkelmans, R., 2014. Flood impacts in Keppel Bay, southern Great Barrier Reef in the aftermath of cyclonic rainfall. PloS ONE. 9, e84739. doi:10.1371/journal.pone.0084739.

Kan, H., Nakashima, Y., Hopley, D., 1997. Coral communities during structural development of a fringing reef flat, Hayman Island, the Great Barrier Reef. Proceedings of the 8th International Coral Reef Symposium, Panama City, Panama. 1, 465-470.

Kelley, R., 2009. Indo Pacific Coral Finder. BYO Guides, Townsville.

Kennedy, D.M., Woodroffe, C.D., 2002. Fringing reef growth and morphology: a review. Earth-Science Reviews. 57, 255-277.

Kittinger, J.N., Pandolfi, J.M., Blodgett, J.H., Hunt, T.L., Jiang, H., Maly, K., McClenachan, L.E., Schultz, J.K., Wilcox, B.A., 2011. Historical reconstruction reveals recovery in Hawaiian coral reefs. PloS One. 6(10): e25460. doi:10.1371/journal.pone.0025460.

Kleypas, J.A., 1996. Coral reef development under naturally turbid conditions: fringing reefs near Broad Sound, Australia. Coral Reefs. 15, 153-167.

Kohler, K.E., Gill, S.M., 2006. Coral Point Count with Excel extensions (CPCe): A visual basic program for the determination of coral and substrate coverage using random point count methodology. Computers and Geosciences. 32, 1259-1269.

Kroon, F.J., Kuhnert, P.M., Henderson, B.L., Wilkinson, S.N., Kinsey-Henderson, A., Abbott, B., Brodie, J.E., Turner, R.D.R., 2012. River loads of suspended solids, nitrogen, phosphorus and herbicides delivered to the Great Barrier Reef lagoon. Marine Pollution Bulletin. 65, 167-181.

Lewis, S.E., Sloss, C.R., Murray-Wallace, C.V., Woodroffe, C.D., Smithers, S.G., 2013. Post-glacial sea-level changes around the Australian margin: a review. Quaternary Science Reviews. 74, 115-138.

Lewis, S.E., Wust, R.A.J., Webster, J.M., Collins, J., Wright, S.A., Jacobsen, G., 2015. Rapid relative sea-level fall along north-eastern Australia between 1200 and 800 cal. yr BP: an appraisal of the oyster evidence. Marine Geology. 370, 20-30.

Lough, J.M., Lewis, S.E., Cantin, N.E., 2015. Freshwater impacts in the central Great Barrier Reef: 1648-2011. Coral Reefs. 34(3), 739-751.

Ludwig, K.R., 2003. Users Manual for Isoplot/Ex version 3.0: A Geochronological Toolkit for Microsoft Excel. Berkeley Geochronology Centre Special Publication No.3. Berkeley.

Maragos, J.E., Evans, C., Holthus, P., 1985. Reef corals in Kaneohe Bay six years before and after termination of sewage discharges (Oahu, Hawaiian Archipelago). Proceedings of the 5th International Coral Reef Congress, Tahiti. 4, 189-194.

McCook, L.J., Jompa, J., Diaz-Pulido, G., 2001. Competition between corals and algae on coral reefs: a review of evidence and mechanisms. Coral Reefs. 19, 400-417.

McCulloch, M., Fallon, S., Wyndham, T., Hendy, E., Lough, J., Barnes, D., 2003. Coral record of increased sediment flux to the inner Great Barrier Reef since European settlement. Nature. 421, 727-730.

McIntyre-Tamwoy, S., 2004. ‘My Barrier Reef’: exploring the Bowen community’s attachment to the Great Barrier Reef. Historic Environment. 17(3), 19-28.

Packett, R., Dougall, C., Ellis, R., Waters, D., Carroll, C., 2014. Modelling reductions of pollutant loads due to improved management practices in the Great Barrier Reef catchments – Mackay Whitsunday NRM Region, Technical Report, Volume 5, Queensland Department of Natural Resources and Mines, Rockhampton, Queensland.

Pandolfi, J.M., Kiessling, W., 2014. Gaining insights from past reefs to inform understanding of coral reef response to global climate change. Current Opinion in Environmental Sustainability. 7, 52-58.

Perry, C.T., Smithers, S.G., 2006. Taphonomic signatures of turbid-zone reef development: Examples from Paluma Shoals and Lugger Shoal, inshore central Great Barrier Reef, Australia. Palaeogeography, Palaeoclimatology, Palaeoecology. 242, 1-20.

Perry, C.T., Smithers, S.G., 2010. Evidence for the episodic “turn on” and “turn off” of turbid-zone coral reefs during the late Holocene sea-level highstand. Geology. 38, 119-122.

Perry, C.T., Smithers, S.G., 2011. Cycles of coral reef ‘turn-on’, rapid growth and ‘turn-off’ over the past 8500 years: a context for understanding modern ecological states and trajectories. Global Change Biology. 17, 76-86.

Perry, C.T., Smithers, S.G., Johnson, K.G., 2009. Long-term coral community records from Lugger Shoal on the terrigenous inner-shelf of the central Great Barrier Reef, Australia. Coral Reefs. 28, 941-948.

Perry, C.T., Smithers, S.G., Roche, R.C., Wassenburg, J., 2011. Recurrent patterns of coral community and sediment facies development through successive phases of Holocene inner-shelf reef growth and decline. Marine Geology. 289, 60-71.

Perry, C.T., Smithers, S.G., Gulliver, P., Browne, N.K., 2012. Evidence of very rapid reef accretion and reef growth under high turbidity and terrigenous sedimentation. Geology. 40(8), 719-722.

Perry, C.T., Steneck, R.S., Murphy, G.N., Kench, P.S., Edinger, E.N., Smithers, S.G., Mumby, P.J., 2015. Regional-scale dominance of non-framework building corals on Caribbean reefs affects carbonate production and future reef growth. Global Change Biology. 21(3), 1153-1164.

Rainford, E.H., 1925. Destruction of the Whitsunday group fringing reefs. Australian Museum Magazine. 2, 175-177.

Richards, H.C., 1938. Some problems of the Great Barrier Reef. University of Queensland Papers, Department of Geology. 1, 68-85.

Roche, R.C., Perry, C.T., Johnson, K.G., Sultana, K., Smithers, S.G., Thompson, A.A., 2011. Mid-Holocene coral community data as baselines for understanding contemporary reef ecological states. Palaeogeography, Palaeoclimatology, Palaeoecology. 299, 159-167.

Roche, R.C., Perry, C.T., Smithers, S.G., Leng, M.J., Grove, C.A., Sloane, H.J., Unsworth, C.E., 2014. Mid-Holocene sea surface conditions and riverine influence on the inshore Great Barrier Reef. The Holocene. 24(8), 885-897.

Rodriguez-Ramirez, A., Grove, C.A., Zinke, J., Pandolfi, J.M., Zhao, J.X., 2014. Coral luminescence identifies the Pacific Decadal Oscillation as a primary driver of river runoff variability impacting the southern Great Barrier Reef. PloS One. 9(1), e84305. doi:10.1371/journal.pone.0084305.

Ryan, E.J., Smithers, S.G., Lewis, S.E., Clark, T.R., Zhao, J.X., 2016a. Chronostratigraphy of Bramston Reef reveals a long-term record of fringing reef growth under muddy conditions in the central Great Barrier Reef. Palaeogeography, Palaeoclimatology, Palaeoecology. 441, 734-747.

Ryan, E.J., Smithers, S.G., Lewis, S.E., Clark, T.R., Zhao, J.X., 2016b. The influence of sea level and cyclones on Holocene reef flat development: Middle Island, central Great Barrier Reef. Coral

Reefs. DOI 10.1007/s00338-016-1453-9.

Saville-Kent, W., 1893. The Great Barrier Reef of Australia. Allen Press, London.

Smithers, S.G., Woodroffe, C.D., 2000. Micro-atolls as sea-level indicators on a mid-ocean atoll. Marine Geology. 168, 61-78.

Smithers, S.G., Hopley, D., Parnell, K.E., 2006. Fringing and nearshore coral reefs of the Great Barrier Reef: Episodic Holocene development and future prospects. Journal of Coastal Research. 22(1), 175-187.

Stanley, G.A.V., 1928. The physiography of the Bowen district and of the northern isles of the Cumberland Group. Reports of the Great Barrier Reef Commission. 2, 1-51.

Steen, R.M., 1972. History of the Port of Bowen: from a paper read to the Bowen Historical Society. Bowen Independent, Bowen.

Steers, J.A., 1937. The coral islands and associated features of the Great Barrier Reefs. The Geographic Journal. 89, 1-28.

Stephenson, W., Endean, R., Bennett, I., 1958. An ecological survey of the marine fauna of Low Isles, Queensland. Australian Journal of Marine and Freshwater Research. 9, 261-329.

Sweatman, H., Delean, S., Syms, C., 2011. Assessing loss of coral cover on Australia's Great Barrier Reef over two decades, with implications for longer-term trends. Coral Reefs. 30, 521-531.

Sweatman, H., Syms, C., 2011. Assessing loss of coral cover on the Great Barrier Reef: A response to Hughes et al. (2011). Coral Reefs. 30, 661-664.

Thompson, A.A., Dolman, A.M., 2010. Coral bleaching: one disturbance too many for near-shore reefs of the Great Barrier Reef. Coral Reefs. 29, 637-648.

Thompson, A., Costello, P., Davidson, J., Schaffelke, B., Uthicke, S., Liddy, M., 2013. Reef Rescue Marine Monitoring Program. Report of AIMS Activities – Inshore coral reef monitoring 2012. Report for Great Barrier Reef Marine Park Authority. Australian Institute of Marine Science, Townsville.

Thurstan, R.H., McClenachan, L., Crowder, L.B., Drew, J.A., Kittinger, J.N., Levin, P.S., Roberts, C.M., Pandolfi, J.M., 2015. Filling historical data gaps to foster solutions in marine conservation. Ocean and Coastal Management. 115, 31-40.

van Woesik, R., Tomascik, T., Blake, S., 1999. Coral assemblages and physico-chemical characteristics of the Whitsunday Islands: evidence of recent community changes. Marine Freshwater Research. 50, 427-440.

Veron, J.E.N, 1986. Corals of Australia and the Indo-Pacific. Australian Institute of Marine Science, Townsville.

Wachenfeld, D., 1997. Long-term trends in the status of coral reef flat benthos: the use of historical photographs. In: Wachenfeld, D., Oliver, J., Davis, K. (Eds.), Proceedings of the State of the Great Barrier Reef World Heritage Area Workshop: 27-29 November 1995, Townsville, Queensland. Great Barrier Reef Marine Park Authority, Townsville, pp. 134-148.

Waterhouse, J., Brodie, J., Lewis, S., Mitchell, A., 2012. Quantifying the sources of pollutants in the Great Barrier Reef catchments and the relative risk to reef ecosystems. Marine Pollution Bulletin. 65, 394-406.

Waters, D.K., Carroll, C., Ellis, R., Hateley, L., McCloskey, J., Packett, R., Dougall, C., Fentie, B., 2014. Modelling reductions of pollutant loads due to improved management practices in the Great Barrier Reef Catchments – Whole of GBR, Volume 1. Department of Natural Resources and Mines. Technical Report (ISBN: 978-1-7423-0999).

Webb, G.E., Nothdurft, L.D., Zhao, Z.X., Opdyke, B., Price, G., 2016. Significance of shallow core transects for reef models and sea-level curves, Heron Reef, Great Barrier Reef. Sedimentology. DOI 10.1111/sed.12266.

Wilkinson, C., 2008. Status of Coral Reefs of the World: 2008. Global Coral Reef Monitoring Network and Reef and Rainforest Research Centre, Townsville, Australia.

Woodroffe, C.D., Kennedy, D.M., Hopley, D., Rasmussen, C.E., Smithers, S.G., 2000. Holocene reef growth in Torres Strait. Marine Geology. 170, 331-346.

Zhao, J.X., Hu, K., Collerson, K.D., Xu, H.K., 2001. Thermal ionization mass spectrometry U-series dating of a hominid site near Nanjing, China. Geology. 29(1), 27-30.

HIGHLIGHTS

- The fringing reefs at Stone Island developed in the early- to mid-Holocene under higher sea level
- The reef flats at Stone Island have not prograded significantly since 4,000 yBP
- Reef flat live coral cover was extremely low at Stone Island (0%) and high at Middle Island (63±20%)
- Inferred changes in reef condition at Stone Island are localised and not regionally evident
- Elevation of the reef flat surface must be considered in photographic comparisons of coral cover